



# Combined dimension reduction and tabulation strategy using ISAT–RCCE–GALI for the efficient implementation of combustion chemistry

Varun Hiremath<sup>a,\*</sup>, Zhuyin Ren<sup>b</sup>, Stephen B. Pope<sup>a</sup>

<sup>a</sup> Cornell University, Mechanical & Aerospace Engineering, Ithaca, NY 14853, USA

<sup>b</sup> ANSYS, Inc., 10 Cavendish Court, Lebanon, NH 03766, USA

## ARTICLE INFO

### Article history:

Received 23 December 2010  
Received in revised form 5 April 2011  
Accepted 11 April 2011  
Available online 12 May 2011

### Keywords:

ISAT  
Dimension reduction  
RCCE  
Greedy algorithm  
PaSR

## ABSTRACT

Computations of turbulent combustion flows using detailed chemistry involving a large number of species and reactions are computationally prohibitive, even on a distributed computing system. Here, we present a new combined dimension reduction and tabulation methodology for the efficient implementation of combustion chemistry. In this study, the dimension reduction is performed using the *rate controlled constrained-equilibrium* (RCCE) method, and tabulation of the reduced space is performed using the *in situ* adaptive tabulation (ISAT) algorithm. The dimension reduction using RCCE is performed by specifying a set of represented (constrained) species, which in this study is selected using a new *Greedy Algorithm with Local Improvement* (GALI) (based on the greedy algorithm). This combined approach is found to be particularly fruitful in the *probability density function* (PDF) approach, wherein the chemical composition is represented by a large number of particles in the solution domain. In this work, the combined approach has been tested and compared to reduced and skeletal mechanisms using a partially-stirred reactor (PaSR) for premixed combustion of (i) methane/air (using the 31-species GRI-Mech 1.2 detailed mechanism and the 16-species ARM1 reduced mechanism) and (ii) ethylene/air (using the 111-species USC-Mech II detailed mechanism, a 38-species skeletal mechanism and a 24-species reduced mechanism). Results are presented to quantify the relative accuracy and efficiency of three different ways of representing the chemistry: (i) ISAT alone (with a detailed mechanism); (ii) ISAT (with a reduced or skeletal mechanism); and (iii) ISAT–RCCE with represented species selected using GALI. We show for methane/air: ISAT (with ARM1 reduced mechanism) incurs 6% error, while ISAT–RCCE incurs the same error using just 8 or more represented species, and less than 1% error using 11 or more represented species, with a twofold speedup relative to using ISAT alone with the GRI-Mech 1.2 detailed mechanism. And we show for ethylene/air: ISAT incurs 7% and 3% errors with the reduced and skeletal mechanisms, respectively, while ISAT–RCCE achieves the same levels of error 7% with just 18 and 3% with just 25 represented species, and also provides 15-fold speedup relative to using ISAT alone with the USC-Mech II detailed mechanism. With fewer species to track in the CFD code, this combined ISAT–RCCE–GALI reduction–tabulation algorithm provides an accurate and efficient way to represent combustion chemistry.

© 2011 The Combustion Institute. Published by Elsevier Inc. All rights reserved.

## 1. Introduction

Modern chemical mechanisms of real fuels involve hundreds or thousands of species and thousands of reactions [1,2]. Incorporating such detailed chemistry in the combustion flow calculations is computationally prohibitive, and thus some form of modelling to reduce the computational cost is inevitable.

In the last two decades or so, numerous dimension reduction techniques have been developed to reduce the computational cost of combustion chemistry. These include:

1. **Skeletal mechanisms:** A skeletal mechanism consists of a selected subset of the species and reactions from the detailed mechanism, and is applicable to within certain accuracy, over the entire range of conditions (e.g., pressures, temperatures, equivalence ratios) of the detailed kinetic mechanism. Many methods have been developed to systematically generate skeletal mechanisms from detailed mechanisms, such as the Directed Relations Graph (DRG) [3], DRG with error propagation (DRGEP) [4] and Simulation Error Minimization Connectivity Method (SEM-CM) [5].
2. **Reduced chemical mechanisms (based on QSSA):** The quasi-steady-state approximation (QSSA) [6,7] has been widely applied to develop reduced chemical mechanisms. The QSSA method involves the identification of QSS species in the system,

\* Corresponding author.

E-mail address: [vh63@cornell.edu](mailto:vh63@cornell.edu) (V. Hiremath).

## Nomenclature

### Roman

$h$	enthalpy
$p$	pressure
$n_e$	number of elements
$n_s$	number of species
$n_{rs}$	number of represented species
$n_{us}$	number of unrepresented species
$n_r$	reduced dimension ( $n_r = n_{rs} + n_e$ )
$\mathbf{w}$	molecular weights of the species
$\mathbf{z}$	species specific moles
$\mathbf{h}$	species molar enthalpies
$\mathbf{h}^f$	species molar enthalpies of formation
$\mathbf{r}$	reduced representation
$\mathbf{z}^r$	specific moles of represented species
$\mathbf{z}^{u,e}$	specific moles of elements in the unrepresented species
$\mathbf{z}^s$	specific moles of species in the skeletal or reduced mechanism
$\mathbf{S}$	chemical production rates
$\mathbf{R}(\mathbf{z}, t)$	reaction mapping after time $t$ starting from $\mathbf{z}$
$\mathbf{B}$	constraint matrix
$\mathbf{E}$	element matrix
$\mathbf{r}(0)$	reduced representation at time $t = 0$
$\mathbf{z}^{CE}(\mathbf{r})$	constrained-equilibrium composition at $\mathbf{r}$
$\mathbf{z}^{DR}(t)$	reaction mapping, $\mathbf{R}(\mathbf{z}^{DR}(0), t)$
$\mathbf{r}^{DR}(t)$	reduced representation after time $t$
$N$	number of test compositions used to compute error

$N_G$	number of test compositions used in the greedy algorithm
$N_L$	number of test compositions used for local improvement in GALI
$N_p$	number of particles in the PaSR
$\Delta t$	reaction time step
$T$	PaSR initial temperature
$S$	size of ISAT table

### Greek

$\Phi$	set of all species
$\Phi^r$	set of represented species
$\Phi^u$	set of unrepresented species
$\Phi^{uu}$	set of undetermined unrepresented species
$\Phi^g$	set of good represented species generated by the greedy algorithm
$\Phi^{gi}$	set of good represented species obtained using GALI
$\epsilon(t, \Phi^r)$	dimension reduction error in the reaction mapping, $\mathbf{R}(\mathbf{z}^{DR}(0), t)$
$\epsilon(\Phi^r)$	error used for defining the optimal set of species
$\phi$	equivalence ratio
$\tau_{res}$	PaSR residence time
$\tau_{mix}$	PaSR mixing time scale
$\tau_{pair}$	PaSR pairing time scale
$\epsilon_{tol}$	ISAT error tolerance

whose net rate of production is assumed to be zero, thereby reducing the governing differential equation for the QSS species into an algebraic relation. These algebraic relations are used to eliminate the QSS species from the system. Reduced mechanisms are generally valid only over a limited range of conditions (i.e., pressures, temperatures, equivalence ratios) compared to skeletal mechanisms.

3. Dimension reduction methods: Another class of dimension reduction techniques is based on the observation that chemical systems involve reactions with a wide range of time scales. As a consequence, reaction trajectories are attracted to lower-dimensional attracting manifolds in the composition space. Computations can be performed in a reduced space by identifying such low-dimensional manifolds, thereby reducing the overall computational cost. Methods based on this idea include rate-controlled constrained equilibrium (RCCE) [8,9], computational singular perturbation (CSP) [10], intrinsic low-dimensional manifolds (ILDm) [11], trajectory-generated low-dimensional manifolds (TGLDM) [12], invariant constrained equilibrium-edge pre-image curve (ICE-PIC) [13] and one-dimensional slow invariant manifold (1D SIM) [14].
4. Storage retrieval methods: In these approaches, combustion chemistry computations are stored in a table, and are used to build inexpensive approximate solutions at a later stage of computation to reduce the overall cost. Methods based on this idea include the structured look-up tabulation [15], repro-modelling [16], artificial neural network (ANN) [17], *in situ* adaptive tabulation (ISAT) [18,19] and piecewise reusable implementation of solution mapping (PRISM) [20].

In recent times, combined methodologies have also been developed, wherein reduced reaction mechanisms or dimension reduction methods are used in conjunction with storage/retrieval methods, such as ISAT-QSSA [21], ISAT-RCCE [22], and recently ICE-PIC with ISAT [23].

In reactive flow calculations, the species concentrations are governed by two processes: chemical reaction and transport. We consider the important class of solution methods in which a splitting scheme is used, where the chemical reaction and transport processes are accounted for in two separate sub-steps.

In the computational modelling of turbulent combustion using PDF methods [24], the fluid composition within the solution domain is represented by a large number of particles. In a full-scale PDF calculation, more than 2 million particles may be used, and the solution can advance for more than 5000 time steps, leading to approximately  $10^{10}$  particle-reaction sub-steps. If such a calculation involves 100 species with the chemistry represented by a detailed mechanism (without reduction or tabulation), then at each reaction sub-step, 100 coupled ODEs need to be solved to determine the species concentrations, which can be very expensive  $\mathcal{O}(0.1)$  s and computationally prohibitive (i.e., 30 years for  $10^{10}$  reaction sub-steps). Instead a dimension reduction method (such as RCCE or ICE-PIC) integrated with ISAT can be used to perform the reactive flow calculations in terms of say 20 represented species; where the combined reduction-storage methodology determines and tabulates (*in situ*) the reduced space in terms of the 20 represented species based on the detailed mechanism. This combined approach can reduce the reaction sub-step time to  $\mathcal{O}(10)$   $\mu$ s giving more than  $10^4$ -fold speedup compared to a direct evaluation using ODE integration (resulting in 30 h for  $10^{10}$  reaction sub-steps).

In our implementation of RCCE, which is integrated with ISAT [13,22,23,25], a specified set of represented (constrained) species is used as constraints to perform dimension reduction. The specification of good constraints is crucial for the accuracy of dimension reduction, and recently we proposed a *greedy algorithm* [26] for selecting good represented species. In this paper we introduce a new *Greedy Algorithm with Local Improvement* (GALI) which can be used to generate an even better set of represented species by further reducing the dimension reduction error obtained by the

greedy algorithm at any given dimension. In this study, we use GALI to select the represented species for performing dimension reduction with RCCE.

The combined reduction–tabulation methodologies primarily involve two errors: (i) the *tabulation* error due to the use of ISAT; and (ii) the *reduction* error due to the use of either a reduced or skeletal mechanism or due to the use of fewer represented species in the dimension reduction methods like RCCE. The tabulation error is controlled by the specified ISAT error tolerance ( $\epsilon_{tol}$ ), and the reduction error is controlled by the number of species retained in the skeletal or reduced mechanism, and by the number of represented species used in the dimension–reduction method. The overall computational cost of course depends on the desired level of accuracy, and the lower the specified error tolerance or the larger the number of represented species, the more is the computational cost. There is a trade-off between accuracy and efficiency, and in this study, we consider a net reduction–tabulation error (defined more precisely in Section 7.3) of about 2% to be an acceptable level of accuracy. We use a low ISAT error tolerance ( $\epsilon_{tol} = 10^{-5}$ ) and select a sufficient number of represented species with GALI to reduce the reduction–tabulation error below 2%.

The outline of the remainder of the paper is as follows: In Section 2 we develop a mathematical representation for a gas-phase reacting system. Next, in Section 3 we describe the partially-stirred reactor (PaSR) which is used for testing the combined dimension reduction and tabulation approach in this study. In the next two Sections 4 and 5 we briefly review the *in situ* adaptive tabulation (ISAT) algorithm and the rate controlled constrained-equilibrium (RCCE) methods. A reader familiar with these concepts may skip these two sections. Following this in Section 6, we present a brief overview of the greedy algorithm and the details of the new GALI. Next, in Section 7 we describe the combined dimension reduction and tabulation methodology. Finally, in Sections 8 and 9 we present the results and draw conclusions.

## 2. Representation of chemistry

We consider a reacting gas-phase mixture consisting of  $n_s$  chemical species, composed of  $n_e$  elements. The set of all species is denoted by  $\Phi$ . The thermo-chemical state of the mixture (at a given position and time) is completely characterized by the pressure  $p$ , the mixture enthalpy  $h$ , and the  $n_s$ -vector  $\mathbf{z}$  of specific moles of the species. (The specific moles of species  $i$  is given as  $z_i = Y_i/w_i = X_i/w_{mix}$ , where  $Y_i$ ,  $X_i$  and  $w_i$  are the mass fraction, mole fraction and molecular weight of the species  $i$ , respectively, and  $w_{mix} \equiv \sum_{i=1}^{n_s} X_i w_i$  is the mixture molecular weight.) To simplify the exposition, we consider an adiabatic and isobaric system with a fixed specified pressure,  $p$ , and so the thermo-chemical state is fully characterized by  $\mathbf{z}$ ,  $h$ .

It is useful to consider the species composition  $\mathbf{z}$  to be an  $n_s$ -vector or a point in the  $n_s$ -dimensional *full composition space*. With  $\mathbf{w}$  denoting the  $n_s$ -vector of molecular weights of all the species, then, for realizability,  $\mathbf{z}$  must satisfy the normalization condition,  $\mathbf{w}^T \mathbf{z} = 1$ . (This corresponds to the species mass fractions summing to unity.)

### 2.1. Reaction trajectories

Due to chemical reactions, the chemical composition  $\mathbf{z}$  evolves in time according to the following set of ordinary differential equations (ODEs)

$$\frac{d\mathbf{z}(t)}{dt} = \mathbf{S}(\mathbf{z}(t)), \quad (1)$$

where  $\mathbf{S}$  is the  $n_s$ -vector of chemical production rates determined by the chemical mechanism used to represent the chemistry.

The *reaction mapping*,  $\mathbf{R}(\mathbf{z}, t)$  is defined to be the solution to Eq. (1) after time  $t$  starting from the initial composition  $\mathbf{z}$ . The reaction mapping obtained by directly integrating the set of ODEs given by Eq. (1) is referred to as a *direct evaluation* (DE). In this study, we use DDASAC [27] for direct evaluation.

## 3. Partially-stirred reactor (PaSR)

We are interested in studying turbulent combustion flow problems using the LES/PDF approach. Computations of turbulent flames using the LES/PDF approach are computationally expensive. To demonstrate the working and efficiency of our combined dimension reduction and tabulation approach, we instead consider the computationally cheaper partially-stirred reactor (PaSR), which is a representative test case for the combustion problems of our interest. A PaSR is similar to a particle PDF method applied to a statistically homogeneous flow. We can vary pressure, inflowing stream temperatures and the reaction time step  $\Delta t$  in the PaSR to be representative of conditions in an LES/PDF calculation.

In this study, we consider the test case of a PaSR involving premixed combustion of two different fuel/air mixtures: (i) methane/air and (ii) ethylene/air.

Unless specified otherwise, the default configuration studied in the PaSR involves two inflowing streams: a stoichiometric premixed stream of given fuel/air mixture at 600 K; and a pilot stream consisting of the adiabatic equilibrium products of the stoichiometric fuel/air mixture (corresponding to unburnt gas temperature of 600 K). The mass flow rates of these streams are in the ratio 0.95:0.05. Initially ( $t = 0$ ), all particle compositions are set to be the pilot-stream composition. The pressure is atmospheric throughout.

Other important parameters involved in the PaSR for the methane/air and ethylene/air premixed combustion cases are listed in the Table 1. The parameters include the equivalence ratio,  $\phi$ ; (unburnt) temperature of the inflowing streams,  $T$ ; pressure,  $p$ ; residence time,  $\tau_{res}$ ; mixing time scale,  $\tau_{mix}$ ; pairing time scale,  $\tau_{pair}$ ; reaction time step,  $\Delta t$ ; number of particles,  $N_p$ ; ISAT error tolerance,  $\epsilon_{tol}$ ; and ISAT table size,  $S$ .

The residence time for methane/air and ethylene/air premixed combustion in PaSR is chosen small enough (relative to the chemical time scale) to introduce a good range of non-equilibrium temperature and species compositions in the PaSR. As the residence time is lowered and approaches the blow-out limit, the PaSR calculations become more computationally intensive. We have tried to maintain a good balance between the computational cost and the range of chemical compositions in the PaSR to perform tests. The temperature distributions inside PaSR for the methane/air and ethylene/air premixed combustion is shown in Figs. 1 and 2, respectively.

The chemical mechanisms used to represent the chemistry for the methane and ethylene fuels are listed in Table 2 along with

**Table 1**

The default values of various PaSR and ISAT parameters used for the methane/air and ethylene/air premixed combustion test cases.

Parameter	Methane/air	Ethylene/air
$\phi$	1	1
$T$	600 K	600 K
$p$	1 atm	1 atm
$\tau_{res}$	10 ms	100 $\mu$ s
$\tau_{mix}$	1 ms	10 $\mu$ s
$\tau_{pair}$	1 ms	10 $\mu$ s
$\Delta t$	0.033 ms	0.33 $\mu$ s
$N_p$	100	100
$\epsilon_{tol}$	$10^{-5}$	$10^{-5}$
$S$	1 GB	1 GB

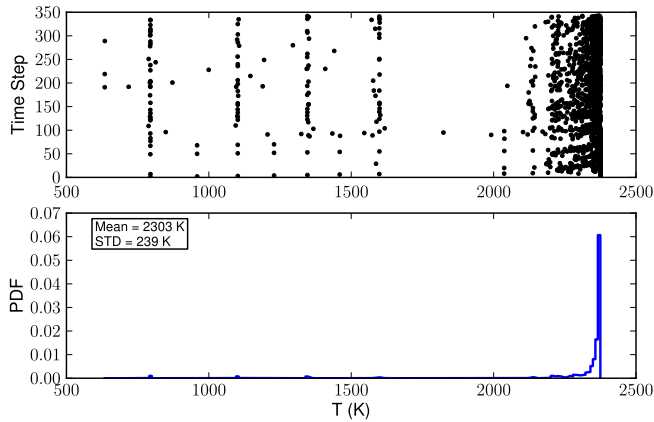


**Fig. 1.** Scatter plot of temperature (top) retrieved from 10 selected particles over 350 time steps and PDF of temperature (bottom) in the statistically stationary state (time steps 100 and above) inside PaSR involving methane/air premixed combustion with residence time  $\tau_{res} = 10$  ms. The equilibrium temperature is 2374 K.

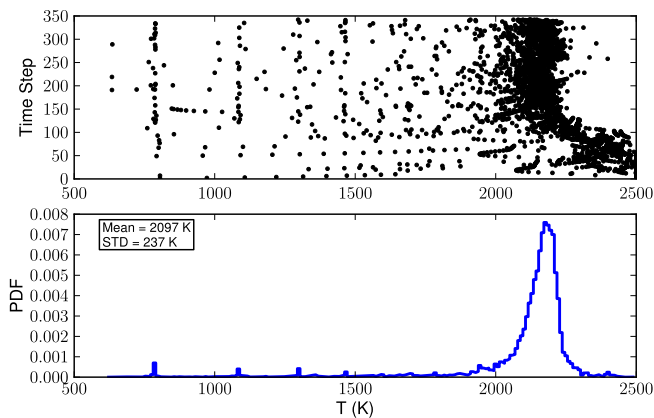


**Fig. 2.** Scatter plot of temperature (top) retrieved from 10 selected particles over 350 time steps and PDF of temperature (bottom) in the statistically stationary state (time steps 100 and above) inside PaSR involving ethylene/air premixed combustion with residence time  $\tau_{res} = 100$   $\mu$ s. The equilibrium temperature is 2500 K.

the details about the number of elements, species and reactions involved in these mechanisms.

In our implementation of PaSR, computations can be performed using the full set of species,  $\Phi$ , in the full composition space (without any dimension reduction) or using a smaller set of represented species,  $\Phi^r$ , using RCCE. For a given test case, PaSR calculations are performed with and without dimension reduction, and the compositions obtained with the two approaches are compared to estimate errors involved in dimension reduction.

In the next two sections we review the concepts of ISAT and RCCE algorithms. A reader familiar with these concepts may skip the next two sections.

## 4. In situ adaptive tabulation (ISAT)

### 4.1. Introduction

ISAT is a tabulation algorithm which returns accurate approximations (within a specified error tolerance) for computationally expensive multi-dimensional functions using (previously evaluated) tabulated function values. The ISAT algorithm has been applied in various fields [28,29], but in particular it has proved to be extremely fruitful in reducing the computational cost of evaluating the reaction mapping in combustion flow problems [19].

**Table 2**

The details of the chemical mechanisms used for methane and ethylene. (The mechanisms with four elements do not include Ar.)

Fuel	Mechanism	Name	Elements	Species	Reactions
Methane	Detailed	GRI-Mech 1.2 [35]	4	31	175
	Reduced	ARM1 [36]	4	16	12-step
Ethylene	Detailed	USC-Mech II (Optimized in 2009) [37,38]	5	111	784
	Skeletal	Skeletal [39] (with Ar added)	5	38	212
	Reduced	Reduced (personal communication, based on [40])	4	24	20-step

### 4.2. Overview of the ISAT algorithm

In this section we briefly describe the key terms involved in the ISAT algorithm which are referred to repeatedly in the following sections.

Consider the application of the ISAT algorithm for the evaluation of reaction mappings in an adiabatic isobaric reactive system with a specified constant pressure,  $p$ , such that the thermo-chemical state is fully characterized by  $\{z, h\}$ . In such a system, given the initial composition  $z(0)$ , enthalpy  $h$ , and the reaction time step  $\Delta t$ , ISAT aims to return the reaction mapping  $z(\Delta t)$  within a specified error tolerance denoted by  $\epsilon_{tol}$ . The initial input composition vector given to ISAT is generally referred to as a *query*, and is denoted by  $\mathbf{x}$ . The query vector  $\mathbf{x}$ , for example, in this case could be of the form

$$\mathbf{x} = \{z(0), h_s(0), \Delta t\}, \quad (2)$$

where  $h_s \equiv h_s(h, z)$  is the sensible enthalpy which is defined as

$$h_s = h - \mathbf{h}^T \mathbf{z}, \quad (3)$$

where  $\mathbf{h}^T$  denotes the  $n_s$ -vector of molar enthalpies of formation of the species.

For this query vector  $\mathbf{x}$ , ISAT returns a mapping, which is denoted by  $\mathbf{f}$ , which is given by

$$\mathbf{f} = \{z(\Delta t), h_s(\Delta t), T(\Delta t)\}, \quad (4)$$

where  $z(\Delta t)$ ,  $h_s(\Delta t)$  and  $T(\Delta t)$  denote the composition vector, the sensible enthalpy and the temperature, respectively, after time step  $\Delta t$ .

Given a query vector  $\mathbf{x}$  to ISAT, a series of steps are followed in the ISAT algorithm to determine the mapping  $\mathbf{f}$ , which are described in detail in [18,19]. Here we list only the important definitions, and key events involved:

1. A stored entry in the ISAT table is referred to as a *leaf*.
2. The region around a leaf's value of  $\mathbf{x}$  in which a linear approximation to  $\mathbf{f}(\mathbf{x})$  can be returned within the specified error tolerance  $\epsilon_{tol}$  is called the *region of accuracy* of that leaf. These regions are approximated by hyper-ellipsoids which are referred to as *ellipsoids of accuracy* (EOA).
3. Given a query  $\mathbf{x}$ , a *search* is performed inside the ISAT table to find an EOA which covers the query point  $\mathbf{x}$ .
4. If such an EOA is found, then a linear approximation to the mapping  $\mathbf{f}(\mathbf{x})$  is returned and this event is referred to as a *successful retrieve*.
5. If the retrieve attempt is unsuccessful, then a direct evaluation of the mapping  $\mathbf{f}(\mathbf{x})$  is performed by integrating Eq. (1).
6. After the direct evaluation, a certain number of leaves close to the query point  $\mathbf{x}$  are selected for grow attempts. If the exact mapping obtained by direct evaluation is found to be within

the specified error tolerance ( $\epsilon_{tol}$ ) of the linear approximation obtained from one of these leaves, then the EOA of that leaf is grown to include the query point  $\mathbf{x}$  and this event is called a *grow*.

7. If all the grow attempts fail, then a new leaf is added to the ISAT table (if not full) and this event is referred to as an *add*.
8. If the table size is full, then  $\mathbf{f}(\mathbf{x})$  is returned without performing an add, and this event is referred to as a *direct evaluation* (DE).

In the present study, ISAT is used to tabulate the reaction mapping,  $\mathbf{R}(\mathbf{z}, t)$ , in the full composition space (without dimension reduction), and also to tabulate the reaction mapping in the reduced space (defined in Section 7.2) when used in conjunction with dimension reduction. In the next section we describe the RCCE dimension reduction method and its implementation.

## 5. Dimension reduction

In this section we briefly describe the notation used in the RCCE dimension reduction method; detailed descriptions are provided in [13,23,26].

In RCCE, the set of species  $\Phi$  is decomposed as  $\Phi = \{\Phi^r, \Phi^u\}$ , where  $\Phi^r$  is the set of *represented* species with cardinality  $n_{rs}$ , and  $\Phi^u$  is the set of *unrepresented* species with cardinality  $n_{us}$ , where  $n_{rs} + n_{us} = n_s$  and  $n_{rs} < n_s - n_e$ .

The *reduced representation* of the species composition is denoted by  $\mathbf{r} \equiv \{\mathbf{z}^r, \mathbf{z}^{u,e}\}$ , where  $\mathbf{z}^r$  is an  $n_{rs}$ -vector of specific moles of represented species,  $\Phi^r$ ; and  $\mathbf{z}^{u,e}$  is an  $n_e$ -vector of specific moles of the elements in the unrepresented species,  $\Phi^u$  (for atom conservation). Thus,  $\mathbf{r}$  is a vector of length  $n_r = n_{rs} + n_e$  in the *reduced composition space*, and the dimension of the system is reduced from  $n_s$  to  $n_r < n_s$ . At any time  $t$ , the reduced representation,  $\mathbf{r}(t)$ , is related to the full composition,  $\mathbf{z}(t)$ , by

$$\mathbf{r}(t) = \mathbf{B}^T \mathbf{z}(t), \quad (5)$$

where  $\mathbf{B}$  is constant  $n_s \times n_r$  matrix which can be determined for a specified set of represented species.

### 5.1. Steps involved in dimension reduction

In this section we briefly describe the four main steps involved in our implementation of RCCE. Since our implementation of RCCE is integrated with ISAT, some of the steps in our implementation of RCCE differ from those of other works found in the literature: those steps are highlighted and justified.

1. The first important step in the application of the RCCE dimension reduction method is the *selection* of the set of represented (constrained) species,  $\Phi^r$ . For a given set of represented species,  $\Phi^r$ , the reduced representation is given as  $\mathbf{r} \equiv \{\mathbf{z}^r, \mathbf{z}^{u,e}\}$ . Alternatively, in many of the RCCE implementations [30,31] general linear constraints on species are specified. In our implementation of RCCE, to simplify the user interface and specification of constraints, we use the species specific moles of the represented species as the constraints.
2. The next step is the *species reconstruction*, i.e., given a reduced representation  $\mathbf{r}(0)$  at time  $t = 0$ , reconstruct an estimate of the full composition denoted by  $\mathbf{z}^{DR}(0)$ .

In RCCE the *species reconstruction* is performed by computing the constrained-equilibrium composition for the given constraints. In our implementation of RCCE, the constrained-equilibrium composition is computed using the CEQ [32] code, with the constraints given by the reduced representation  $\mathbf{r}$ . The constrained-equilibrium composition at  $\mathbf{r}$  is denoted by  $\mathbf{z}^{CE}(\mathbf{r})$ . So the reconstructed composition in RCCE is given as

$$\mathbf{z}^{DR}(0) = \mathbf{z}^{CE}(\mathbf{r}(0)). \quad (6)$$

3. The next step is to obtain the *reaction mapping*. Starting from the reconstructed composition,  $\mathbf{z}^{DR}(0)$ , the set of ODEs (1) is integrated numerically in the full space using DDASAC [27] to obtain the reaction mapping after time  $t$ , denoted by  $\mathbf{z}^{DR}(t)$ , as shown in Fig. 1 in [26].

A different approach for the RCCE method as suggested in [9] and also used in [30,31] is to integrate the rate equations for the constraint potentials which is more economical than integrating the ODEs (1) directly. In our implementation of RCCE, we chose the former approach for the ease of combining RCCE dimension reduction method with ISAT, which is discussed in more detail in [22]. It should be noted that the reaction mappings obtained using these two approaches are not the same, and they actually provide two different approximations to the exact reaction mapping.

4. The final step involved in the dimension reduction method is *reduction*, i.e., from the obtained *reaction mapping* after time  $t$ ,  $\mathbf{z}^{DR}(t)$ , compute the *reduced representation* denoted by  $\mathbf{r}^{DR}(t)$  (shown in Fig. 1 in [26]), given as:

$$\mathbf{r}^{DR}(t) = \mathbf{B}^T \mathbf{z}^{DR}(t). \quad (7)$$

To summarize, the key steps involved in the RCCE dimension reduction method are

1. *Selection*: Identifying good constraints or the set of represented species,  $\Phi^r$  for dimension reduction.
2. *Species reconstruction*: Given the constraints,  $\mathbf{r}(0)$ , reconstructing the full composition,  $\mathbf{z}^{DR}(0)$ .
3. *Reaction mapping*: Starting from the *reconstructed composition*  $\mathbf{z}^{DR}(0)$ , computing the *reaction mapping* after time  $t$  in the full composition space  $\mathbf{z}^{DR}(t)$ .
4. *Reduction*: From the *reaction mapping*  $\mathbf{z}^{DR}(t)$ , obtaining the *reduced representation*  $\mathbf{r}^{DR}(t)$  after time  $t$ .

### 5.2. Dimension reduction errors

In this section we define the various errors involved in the dimension reduction process and describe the method employed to measure these errors using the PaSR.

Given a composition,  $\mathbf{z}(0)$  in the full composition space, the *reaction mapping*,  $\mathbf{R}(\mathbf{z}(0), t)$  (for  $t \geq 0$ ) is more concisely denoted by  $\mathbf{z}(t)$  (see Fig. 4 in [26]).

For a given set of *represented* species,  $\Phi^r$ , the *reduced representation* of the full composition,  $\mathbf{z}(0)$  is denoted by  $\mathbf{r}(0)$  and is obtained by performing the *reduction* using (5) as

$$\mathbf{r}(0) = \mathbf{B}^T \mathbf{z}(0). \quad (8)$$

At  $\mathbf{r}(0)$ , the reconstructed composition using a dimension reduction method is denoted by  $\mathbf{z}^{DR}(0)$ . Starting from the reconstructed composition, the *reaction mapping*,  $\mathbf{R}(\mathbf{z}^{DR}(0), t)$  in the full composition space is more concisely denoted by  $\mathbf{z}^{DR}(t)$  (see Fig. 4 in [26]).

Now for a representative test problem, to estimate the errors incurred using a dimension reduction method, a number of test compositions are selected in the full space. Let the number of test composition used be denoted by  $N$ . To generate those test compositions, we perform a PaSR computation in the *full composition space* (without dimension reduction) and then pick  $N$  distinct test compositions (corresponding to *adds* in the ISAT table) in the full space and denote them by  $\mathbf{z}^{(n)}(0)$ , for  $n = 1$  to  $N$ ; and their corresponding *reaction mappings* after a fixed constant time  $t$  are denoted by  $\mathbf{z}^{(n)}(t)$ .

At the  $N$  chosen compositions,  $\mathbf{z}^{(n)}(0)$ , in the full space, and for a given set of *represented* species,  $\Phi^r$ , we denote the corresponding

reduced representations by  $\mathbf{r}^{(n)}(0)$ , the reconstructed compositions by  $\mathbf{z}^{DR(n)}(0)$ , and the reaction mappings by  $\mathbf{z}^{DR(n)}(t)$ .

Note that, given  $\mathbf{z}(0)$  and  $t$ ,  $\mathbf{z}^{DR}(t)$  depends on the specification of the represented species,  $\Phi^r$ . As needed, we show this dependence explicitly by the notation  $\mathbf{z}^{DR}(t, \Phi^r)$ .

At this stage, we define the error in the *reaction mapping* obtained after time  $t$  starting from the reconstructed composition to be

$$\epsilon(t, \Phi^r) = \frac{[\mathbf{z}^{DR(n)}(t, \Phi^r) - \mathbf{z}^{(n)}(t)]_{rms}}{[\mathbf{z}^{(n)}(t)]_{rms}}, \quad (9)$$

where the operator  $[\ ]_{rms}$  is defined by, for example,

$$[\mathbf{z}^{(n)}(t)]_{rms} = \sqrt{\frac{1}{N} \sum_{n=1}^N \|\mathbf{z}^{(n)}(t)\|^2}, \quad (10)$$

where  $\|\mathbf{z}\|$  denotes the 2-norm.

In particular we have two important errors in the dimension reduction method corresponding to  $t = 0$  and  $t = \Delta t$ :

1. *Species reconstruction error*: This is the error in reconstructing the full composition given a reduced composition  $\mathbf{r}(0)$  at  $t = 0$  and is given by Eq. (9) as  $\epsilon(0, \Phi^r)$ .
2. *Reaction mapping error*: This is the error in the reaction mapping obtained after time step  $\Delta t$  (reaction time step) starting from the reconstructed composition and is equal to  $\epsilon(\Delta t, \Phi^r)$ .

## 6. Selection of represented species

In the RCCE dimension reduction method, the selection of represented species for dimension reduction is an important task. In many of the RCCE applications, the constraints are found by a careful examination of the chemical reactions involved in the system [30,31,33]. Ideally one would like to find the *optimal* set of represented species that produces the minimum dimension reduction error, but finding such an optimal set of species is very difficult. Recently we proposed a new automated *greedy algorithm* [26] for selecting represented species for the RCCE dimension reduction method, which showed promising results. Based on this greedy algorithm, we have now developed a new *Greedy Algorithm with Local Improvement* (GALI) which performs even better than the original greedy algorithm proposed in [26]. In the following sections, we briefly review the greedy algorithm and then present details about the GALI.

### 6.1. Greedy algorithm

A greedy algorithm proceeds in stages, making the best (locally optimum) choice at each stage while finding a solution [34]. Greedy algorithms are not guaranteed to give the optimal solutions, but provide good solutions for many mathematical problems.

In our greedy algorithm [26], we split the task of selecting  $n_{rs}$  number of represented species into  $n_{rs}$  different stages, selecting the best available species (one which minimizes the error) at each stage. In [26], results are reported of RCCE dimension reduction tests using the greedy algorithm for PaSR computations involving methane/air premixed combustion at many equivalence ratios, pressures and temperatures. The main conclusion drawn from the results presented in [26] is that the greedy algorithm works well at small values of  $n_{rs}$  (say  $\leq 5$ ), but at higher values of  $n_{rs}$ , the greedy algorithm is found to generate a poor set of represented species in some cases.

As an attempt to further reduce the error obtained with the greedy algorithm at high values of  $n_{rs}$ , we have introduced an additional *local improvement* step to the greedy algorithm which is described in the next section.

### 6.2. Greedy Algorithm with Local Improvement (GALI)

We present a new method for further improving the dimension reduction error of the set of represented species obtained by the greedy algorithm. This is achieved by performing a *local improvement* over the set of species selected by the greedy algorithm at any given dimension.

In the greedy algorithm, at each stage, one new species (producing the minimum error) is added to the set of species selected in the previous stages. The greedy algorithm does not allow for a species selected in the previous stages to be “swapped” with another species producing lower error. For this reason, a new local improvement step has been introduced in the greedy algorithm to enable replacement of previously selected species in the greedy algorithm by species which result in lower error. The idea behind the local improvement step is to sequentially swap a species from the set of represented species obtained from the greedy algorithm by a species from the set of unrepresented species (one at a time) and check for improvement in error. (Only single species swaps are considered to reduce the overall computations involved in the local improvement step.) In the local improvement step, all possible species swaps between the represented and the unrepresented set of species are performed to check for improvement in error. Any species swap that results in improvement in error is saved, and at the end of the local improvement step a new improved set of species (with an error less than or equal to the error given by the greedy algorithm) is generated.

The complete algorithm of first applying the greedy algorithm and later improving the set of represented species by performing local improvement is called the *Greedy Algorithm with Local Improvement* (GALI).

The greedy algorithm is described in detail in [26]. Here we present the algorithm for the local improvement step. In the greedy algorithm a fixed number of test points,  $N = N_G$ , are used to compute the error. The local improvement step described here can be applied using a fewer number of test points,  $N = N_L$ , such that  $N_L < N_G$ , to reduce the computational cost. To explicitly specify the number of test points used for computing the error, here we use the notation  $\epsilon(N, t, \Phi^r)$  to denote the error (Eq. (9)) computed using  $N$  test points. For a given definition of error – species reconstruction with  $t = 0$  or reaction mapping error with  $t = \Delta t$  – we denote the error more concisely as  $\epsilon(N, \Phi^r)$ .

Following the notation used in [26], the local improvement step at a given value of  $n_{rs}$  can be performed as follows:

1. Apply the greedy algorithm based on the given definition of error,  $\epsilon(N_G, \Phi^r)$ , and obtain the set of  $n_{rs}$  represented species denoted by  $\Phi^r$ .
2. Let the set of represented species at any stage of the local improvement algorithm be denoted by  $\Phi^r$ . Initially,  $\Phi^r = \Phi^g$ . At any stage the set of undetermined unrepresented species is denoted by  $\Phi^{uu}(\Phi^r)$ .
3. Let the set of species obtained at the end of the local improvement step be denoted by  $\Phi^{gl}$ . Initially, we set  $\Phi^{gl} = \Phi^g$  (assuming no improvement).
4. Let  $\Phi_{jk}^r$  denote the set of species obtained by swapping the  $j^{th}$  species from  $\Phi^r$  with the  $k^{th}$  species from  $\Phi^{uu}(\Phi^r)$ .
5. We use  $N_L$  test points inside the local improvement step to compute error. The local improvement step involves the following loop:
  - for  $j$  from 1 to cardinality of  $\Phi^r$
  - for  $k$  from 1 to cardinality of  $\Phi^{uu}(\Phi^r)$
  - \* form the set  $\Phi_{jk}^r$  and evaluate  $\epsilon(N_L, \Phi_{jk}^r)$
  - \* if  $\epsilon(N_L, \Phi_{jk}^r) < \epsilon(N_L, \Phi^r)$  then reset  $\Phi^r = \Phi_{jk}^r$
  - end for
  - end for

6. If  $\Phi^r \neq \Phi^{gi}$ , then save the set of species,  $\Phi^{gi} = \Phi^r$ , and rerun the previous local improvement loop (5), else continue.
7. Check if  $\Phi^{gi}$  generates lower error than  $\Phi^g$  over the  $N_G$  test points used in the greedy algorithm. If  $\epsilon(N_G, \Phi^{gi}) < \epsilon(N_G, \Phi^g)$ , then save  $\Phi^{gi}$  else reset  $\Phi^{gi} = \Phi^g$ .

In the above algorithm, the local improvement loop (steps 5 and 6) is guaranteed to terminate because of the strictly non-increasing error check being employed. In all the cases tested, the local improvement loop has never been executed for more than three times. If needed, an upper bound can also be set on the maximum number of times the local improvement loop can be executed.

At the end of the local improvement step, we obtain an improved set of species with an error less than or equal to the error obtained by the greedy algorithm.

### 6.3. Computational cost

The computational cost of the greedy algorithm and the local improvement step directly depends on the number of computations involved in the evaluation of errors. For a fixed value of  $n_{rs}$ , the number of computations involved are

- greedy algorithm:  $\mathcal{O}(n_{rs}n_sN_G)$ ; and
- local improvement:  $\mathcal{O}(n_{rs}(n_s - n_{rs})N_LM)$ ,

where  $M$  is the average number of local improvement loops executed.

More quantitative results for the computational cost of the greedy algorithm and local improvement are presented in the next section.

### 6.4. Comparison of results

In this section we present results comparing dimension reduction error obtained by the greedy algorithm and the improvements achieved by the local improvement step.

We consider the PaSR with methane/air premixed combustion and study two cases for which the greedy algorithm does not yield very good results (as presented in [26]):

1.  $\phi = 1.2$ ,  $T = 1200$  K and  $p = 1$  atm;
2.  $\phi = 0.8$ ,  $T = 1200$  K and  $p = 1$  atm,

where  $\phi$  is the equivalence ratio,  $T$  is the temperature of the inflowing premixed stream and  $p$  is the pressure inside the PaSR.

For the above two cases we first apply the greedy algorithm for  $n_{rs} = 1$ –15 and obtain the represented species ordering. Next, we apply the local improvement step (as described in the previous section) over the species set obtained from the greedy algorithm for  $n_{rs} = 3$ –15. We skip  $n_{rs} = 1$  which is already the optimal, and  $n_{rs} = 2$  where the local improvement is not expected to give any further improvement.

The dimension reduction error for case (1)  $\phi = 1.2$ ,  $T = 1200$  K and  $p = 1$  atm is shown in Fig. 3 and for case (2)  $\phi = 0.8$ ,  $T = 1200$  K and  $p = 1$  atm is shown in Fig. 4. In these figures, we see that the local improvement step reduces the error at many values of  $n_{rs}$ . In case (2), the greedy algorithm already performs quite well (error is less than  $10^{-4}$  for  $n_{rs} > 12$ ), so in Fig. 4 we do not see significant improvement with the local improvement step, however in case (1), the greedy algorithm performs poorly (error remains constant at about  $10^{-2}$  for  $n_{rs} > 4$ ), and so in Fig. 3 we see more than an order of magnitude reduction in error for  $n_{rs} > 10$ . In the figures, at each value of  $n_{rs}$ , the reduction in error achieved at the end of each local improvement loop is marked. We see that

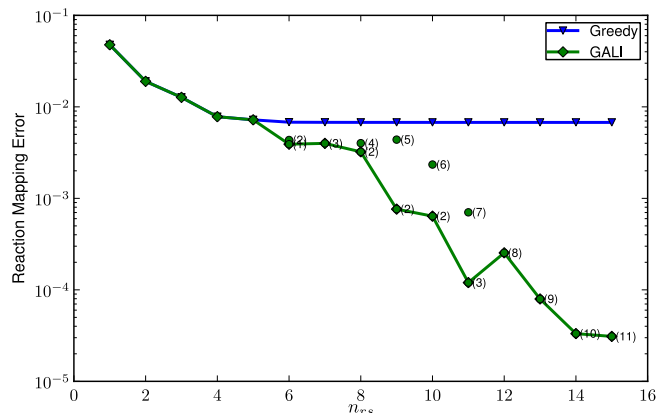


**Fig. 3.** Reaction mapping error for methane/air premixed combustion at  $\phi = 1.2$ ,  $T = 1200$  K and  $p = 1$  atm as a function of number of represented species,  $n_{rs}$ , obtained with (i) Greedy algorithm (using  $N_G = 2500$  test points) and (ii) GALI (using  $N_L = 200$  test points for local improvement). At each value of  $n_{rs}$ , the error achieved after each local improvement loop in the GALI algorithm is marked with a solid circle and the number of successful swaps (resulting in reduction in error) performed in that loop are indicated in parenthesis. The test points are selected from a PaSR run involving methane/air premixed combustion at  $\phi = 1.2$ ,  $T = 1200$  K and  $p = 1$  atm with chemistry represented by the 31-species GRI-Mech 1.2 detailed mechanism.

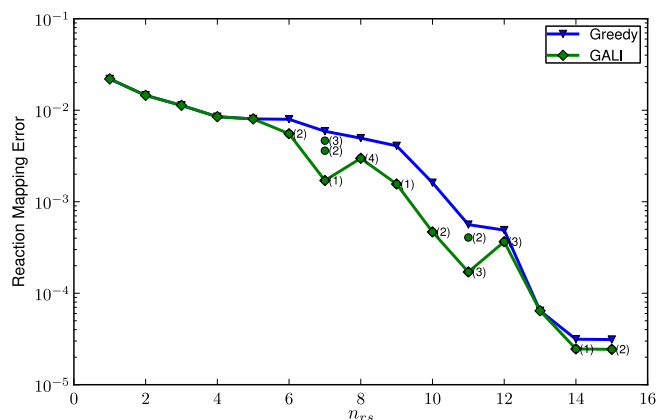


**Fig. 4.** Reaction mapping error for methane/air premixed combustion at  $\phi = 0.8$ ,  $T = 1200$  K and  $p = 1$  atm as a function of number of represented species,  $n_{rs}$ , obtained with (i) Greedy algorithm (using  $N_G = 2500$  test points) and (ii) GALI (using  $N_L = 200$  test points for local improvement). At each value of  $n_{rs}$ , the error achieved after each local improvement loop in the GALI algorithm is marked with a solid circle and the number of successful swaps (resulting in reduction in error) performed in that loop are indicated in parenthesis. The test points are selected from a PaSR run involving methane/air premixed combustion at  $\phi = 0.8$ ,  $T = 1200$  K and  $p = 1$  atm with chemistry represented by the 31-species GRI-Mech 1.2 detailed mechanism.

at any  $n_{rs}$  value, no more than three loops of local improvement are executed.

The total CPU time taken for the greedy, local improvement and the overall GALI for case (1) is shown in Fig. 5. (The CPU times for case (2) are similar and hence are not shown.) We see that the greedy algorithm takes approximately 20 min per species selection. The local improvement takes approximately the same order of time as the greedy algorithm at all the values of  $n_{rs}$ . The combined cost of the GALI is therefore approximately twice the cost (40 min per species selection) of the greedy algorithm, but the cost is still linear in the number of represented species  $n_{rs}$ .

Note that here the cost of GALI has been computed for all the values of  $n_{rs}$ , and the CPU time taken at  $n_{rs} = 26$  is about 20 h. However,

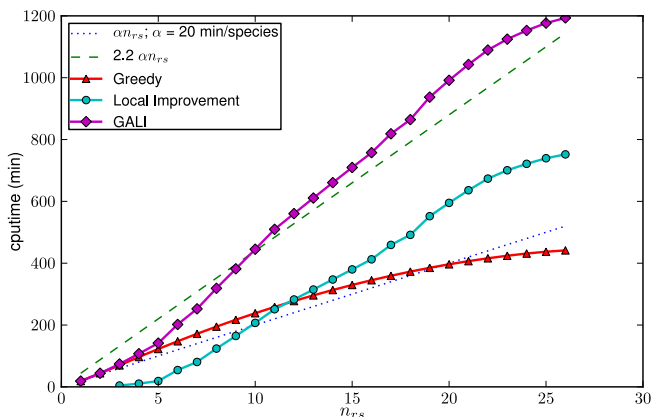


**Fig. 5.** The CPU time spent in selecting represented species based on the reaction mapping error (i) using the greedy algorithm (with  $N_C = 2500$  test points); (ii) performing local improvement (with  $N_L = 200$  test points); and (iii) using complete GALI at different values of  $n_{rs}$ . The test points are selected from a PaSR run involving methane/air premixed combustion at  $\phi = 1.2$ ,  $T = 1200$  K and  $p = 1$  atm with chemistry represented by the 31-species GRI-Mech 1.2 detailed mechanism. The CPU time is measured by running a serial implementation of the greedy algorithm on a 2.2 GHz Quad-Core AMD Opteron(tm) Processor.

- for sufficient accuracy,  $n_{rs} = 15$  is adequate, and the CPU time for GALI at  $n_{rs} = 15$  is around 10 h;
- GALI needs to be applied only once (for one set of conditions and a specified value of  $n_{rs}$ ) and the same set of species is likely to be good in other conditions [26]. (In [26] we have already shown that species selected at one condition work well at other conditions, and with the addition of the local improvement step, the combined GALI may work well over a wider range of conditions.); and
- the cost of GALI is small compared to the savings achieved when applied to LES/PDF which require  $10^4$ – $10^5$  CPU h.

In short, the local improvement step can be used to reduce errors in cases where the greedy algorithm alone may not yield very good results.

## 7. Combined dimension reduction and tabulation

In the previous two sections we described the tabulation algorithm using ISAT and dimension reduction using RCCE. Both the methodologies are very good in reducing the computational cost of combustion chemistry in their own perspectives, but when combined they can reduce the cost even further.

### 7.1. Introduction

The ISAT algorithm has been successfully applied in combustion chemistry problems involving up to  $n_s \leq 50$  species. For problems in higher dimensions, i.e. problems involving more than 50 species, the direct use of ISAT may not be very efficient, due to the large table size and search times. Similarly, dimension reduction can be used to represent the chemistry using a reduced number of species, thereby reducing the cost of tracking species in a CFD code. But, if a tabulation algorithm is not used in conjunction, the dimension reduction alone cannot be very efficient due to the expensive species reconstruction and reaction mapping involved in the algorithm (as described in Section 5) for computing the reduced mapping. Our task is to integrate these two successful methodologies – tabulation and dimension reduction – to extract the maximum out of both and make the combined algorithm accurate and efficient for combustion chemistry problems.

In this combined strategy of dimension reduction and tabulation, we first apply the dimension reduction method using RCCE by specifying a set of represented species (selected using the GALI algorithm) and then we tabulate the reduced space using ISAT. This combined methodology can be applied to chemical systems involving a large number of species (100–1000) by first applying the dimension reduction to reduce the dimensionality of the system to say around 20 (depending on the level of accuracy needed) and then using the ISAT to tabulate the reaction mapping in the reduced space. (For very large mechanisms involving more than 1000 species, it may be more appropriate to use the ISAT–RCCE–GALI approach on a smaller skeletal mechanism, which of course will be less accurate but may be computationally more feasible.) Since the tabulation is done over the reduced space in a lower dimension, retrieving from the ISAT table is very efficient. However, since the reaction mapping is computed in the full space, constructing the ISAT table may be relatively costly. Nevertheless, for problems such as LES/PDF computation requiring very many queries, the overall efficiency may be significantly improved.

### 7.2. Combined reduction–tabulation algorithm

A simplified schematic of the combined dimension reduction and tabulation algorithm is shown in Fig. 6. The first step (pre-processing) in this combined reduction–tabulation approach is the specification of the represented species for dimension reduction. Given the number of constrained species  $n_{rs}$ , or a dimension reduction error tolerance  $\epsilon_{DR,tol}$ , we apply GALI (using a representative PaSR configuration) to obtain the specified number of represented species or enough number of represented species such that the dimension reduction error (Eq. (9)) is less than the specified error tolerance. Given the represented species, the reduced representation is defined as  $\mathbf{r} \equiv \{\mathbf{z}^r, \mathbf{z}^{u,e}\}$ .

In an isobaric adiabatic system with a specified fixed pressure,  $p$ , the chemistry is represented using this combined approach by the reduced set of variables,  $\{\mathbf{r}, h\}$ . So, the only variables that need to be stored and carried (for example by the particles in a PDF simulation) are the reduced variables,  $\mathbf{r}$  and  $h$ . Given the initial reduced composition  $\mathbf{r}(0)$ , the mapping after time step  $\Delta t$  is given (as described in Section 5.1 and shown in Fig. 6) by first performing species reconstruction to obtain  $\mathbf{z}^{DR}(0)$ , followed by computing the reaction mapping  $\mathbf{z}^{DR}(\Delta t)$  and then performing the reduction to retrieve  $\mathbf{r}(\Delta t) \equiv \mathbf{r}^{DR}(\Delta t)$ . Computing the exact mapping with dimension reduction is even more expensive than computing the reaction mapping in the full composition space (i.e., getting  $\mathbf{z}(\Delta t)$  from  $\mathbf{z}(0)$ ) due to the additional species reconstruction and reduction steps involved. So dimension reduction alone is not very efficient, except for the fact that the total number of variables that need to be carried in the CFD code is reduced, and so fewer scalar equations need to be solved in the CFD code.

The dimension reduction when integrated with ISAT becomes much more efficient. In addition to performing dimension reduction, the reduced mappings,  $\mathbf{r}(\Delta t)$  are tabulated using ISAT. In this case, the query vector to ISAT is given as

$$\mathbf{x} = \{\mathbf{r}(0), h_s^n(0), \Delta t\}, \quad (11)$$

where  $h_s^n \equiv h_s^n(h, \mathbf{r})$  is the nominal sensible enthalpy defined only in terms of the reduced variables  $\mathbf{r}$ , for example, as

$$h_s^n \equiv h - \mathbf{h}^{f,r} \mathbf{z}^r, \quad (12)$$

where  $\mathbf{h}^{f,r}$  denotes the  $n_{rs}$ -vector of molar enthalpies of formation of the represented species.

The mapping obtained from ISAT is given as

$$\mathbf{f} = \{\mathbf{r}(\Delta t), h_s^n(\Delta t), T^a(\Delta t)\}, \quad (13)$$

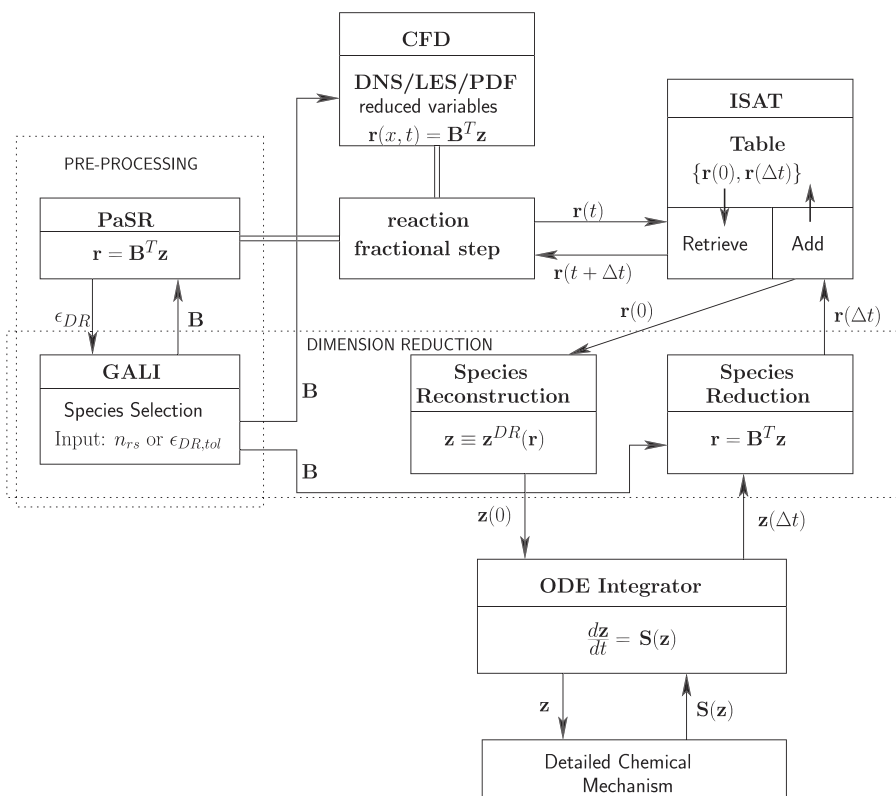


**Fig. 6.** Schematic of the combined dimension reduction and tabulation algorithm. The pre-processing step involves the selection of represented species using GALI with a representative PaSR test problem for a specified number of represented species,  $n_{rs}$ , or a specified dimension reduction error tolerance,  $\epsilon_{DR,tol}$ . The choice of represented species is encapsulated in the specification of the  $n_s \times n_r$  matrix  $\mathbf{B}$ , which relates the reduced composition  $\mathbf{r}$  to the full composition  $\mathbf{z}$  by  $\mathbf{r} = \mathbf{B}^T \mathbf{z}$ . At each reaction fractional step, ISAT is invoked to retrieve the reduced mapping  $\mathbf{r}(\Delta t)$ . For an unsuccessful retrieve, the reduced mapping is obtained using RCCE by performing species reconstruction (using CEQ [32]), followed by computing the reaction mapping with the detailed mechanism (using DDASAC [27]), followed by reduction to obtain  $\mathbf{r}(\Delta t)$ .

where  $T^a(\Delta t)$  denotes an approximated temperature after time step  $\Delta t$ . (In Fig. 6, instead of  $\mathbf{x}$  and  $\mathbf{f}$  we only show  $\mathbf{r}(0)$  and  $\mathbf{r}(\Delta t)$  for brevity.) Since with dimension reduction the composition of only the represented species is stored in the ISAT table, the thermodynamic variables like temperature and density need to be approximated using the reduced representation, which is explained in more detail in the Appendix A.

In the combined approach shown in Fig. 6, the exact mapping is computed only when a *grow* or *add* is performed in ISAT. For a successful retrieve, the reduced mapping is returned directly using the stored information in ISAT. Since the size of the query vector  $\mathbf{x}$  and the mapping vector  $\mathbf{f}$  are smaller, the ISAT table size is also smaller, thus resulting in faster search and retrieve times.

To summarize, the combined dimension reduction and tabulation strategy has the following advantages:

1. Fewer species need be carried and solved for in the CFD code – a significant reduction in computational cost.
2. The ISAT table size is relatively smaller, leading to faster search and query time.

### 7.3. Reduction–tabulation error

In this study, we compare the accuracy and performance of the following three methodologies for representing chemistry:

1. ISAT: using ISAT directly to tabulate chemistry with a detailed chemical mechanism (without any dimension reduction)
2. ISAT + SKELETAL/REDUCED: using ISAT to tabulate chemistry with a skeletal or reduced chemical mechanism

3. ISAT + RCCE: using the combined ISAT–RCCE reduction–tabulation algorithm with represented species selected using GALI

The primary quantity of interest is the accuracy of the *reaction mapping* obtained using these three different methodologies. We compute the error involved in these three methods by considering the error in the reaction mapping obtained using these methods relative to a direct evaluation using ODE integration with the detailed mechanism. The reaction mappings obtained using an ODE integrator (we use DDASAC [27] in this work) typically involve very small errors (relative to these methods) and hence can be deemed accurate. We refer to the error involved in these methods as the *reduction–tabulation error*, which for a direct use of ISAT with a detailed mechanism reduces to simply *tabulation error* (as there is no reduction involved).

We measure the reduction–tabulation error using the PaSR test setup. We first perform PaSR calculations in the full composition space (without dimension reduction) using the detailed mechanism and store particle compositions and their reaction mappings computed using direct evaluation (with DDASAC) after each reaction sub-step. Let the stored initial particle composition be denoted by  $\mathbf{z}^{(n)}(0)$  and its mapping (after time step  $\Delta t$ ) by  $\mathbf{z}^{(n)}(\Delta t)$  for  $n = 1-N$ , where  $N$  denotes the total number of stored compositions and their reaction mappings. We also store the initial enthalpy  $h^{(n)}(0)$ , and initial temperature  $T^{(n)}(0)$  (corresponding to  $\mathbf{z}^{(n)}(0)$ ), which are needed for computing the reaction mapping in the aforementioned reduction–tabulation methodologies.

Using these stored compositions, the reduction–tabulation error is computed by considering the error in the reaction mapping obtained using one of the three aforementioned methods. At the stored compositions, we first obtain the composition of the

represented species used under the considered method. We denote (see Fig. 7) the reduced representation corresponding to  $\mathbf{z}^{(n)}(0)$  by  $\mathbf{z}^{r(n)}(0)$  and that corresponding to  $\mathbf{z}^{(n)}(\Delta t)$  by  $\mathbf{z}^{r(n)}(\Delta t)$ . The reaction mapping starting from  $\mathbf{z}^{r(n)}(0)$  obtained by the considered reduction–tabulation (RT) method is denoted by  $\mathbf{z}_{RT}^{r(n)}(\Delta t)$ .

The reduction–tabulation error, denoted by  $\epsilon_{RT}$ , is then given as

$$\epsilon_{RT} = \frac{[\mathbf{z}^r(\Delta t) - \mathbf{z}_{RT}^r(\Delta t)]_{rms}}{[\mathbf{z}^r(\Delta t) - \mathbf{z}^r(0)]_{rms}}, \quad (14)$$

where the operator  $[\ ]_{rms}$  is defined previously in Eq. (10).

In particular, for the three aforementioned methods, the involved reduced compositions are given as follows:

1. ISAT: since no reduction is involved in this case, we have

$$\mathbf{z}^r(0) \equiv \mathbf{z}(0), \quad \mathbf{z}^r(\Delta t) \equiv \mathbf{z}(\Delta t) \quad \text{and} \quad \mathbf{z}_{RT}^r(\Delta t) \equiv \mathbf{z}_{ISAT}(\Delta t), \quad (15)$$

where  $\mathbf{z}_{ISAT}(\Delta t)$  denotes the reaction mapping obtained from ISAT (see Fig. 7). The error computed for this case is referred to as the *tabulation error*.

2. ISAT + SKELETAL/REDUCED: in this case, we need to obtain the composition of the species involved in the skeletal or reduced mechanism from the stored full compositions,  $\mathbf{z}(t)$ . Let  $\mathbf{z}^s(t) \equiv \mathbf{z}^s(\mathbf{z}(t))$  denote the concentration of species in the skeletal mechanism obtained from the full composition,  $\mathbf{z}(t)$ , then we define

$$\mathbf{z}^r(t) \equiv \mathbf{z}^s(t) / (\mathbf{w}^{s^T} \mathbf{z}^s(t)), \quad (16)$$

where  $\mathbf{w}^s$  denotes molecular weights of the species in the skeletal mechanism, and  $\mathbf{z}^s(t)$  is normalized to satisfy the realizability condition,  $\mathbf{w}^{s^T} \mathbf{z}^s = 1$ . The reaction mapping,  $\mathbf{z}_{RT}^r(\Delta t)$ , is computed (using the skeletal mechanism) starting from  $\mathbf{z}^r(0)$  with the same initial temperature as  $\mathbf{z}(0)$ .

3. ISAT + RCCE: in this case, for the given set of represented species selected using GALI, the reduced representation is simply the concentration of the represented species denoted by  $\mathbf{z}^r$ . The reaction mapping  $\mathbf{z}_{RT}^r(\Delta t)$  is obtained using the combined reduction–tabulation algorithm with ISAT–RCCE (see Fig. 7).

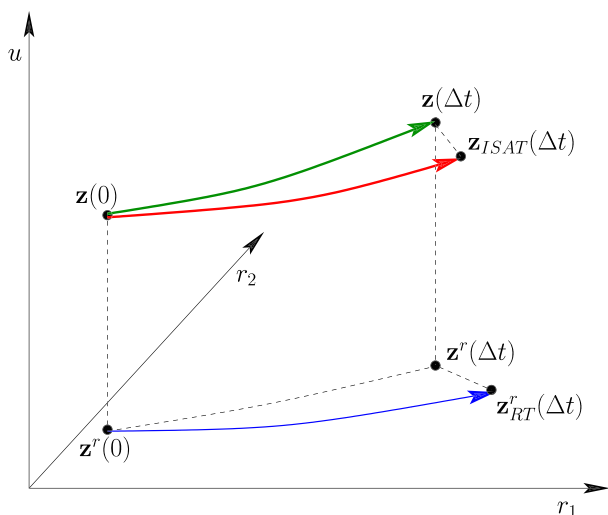


**Fig. 7.** The various compositions involved in the computation of reduction–tabulation error.  $\mathbf{z}(0)$  denotes an initial composition in the full space.  $\mathbf{z}(\Delta t)$  and  $\mathbf{z}_{ISAT}(\Delta t)$  denote the reaction mappings obtained with direct evaluation (using DDASAC) and ISAT, respectively in the full composition space using the detailed mechanism. The composition of the represented species at  $\mathbf{z}(0)$  is denoted by  $\mathbf{z}^r(0)$  and at  $\mathbf{z}(\Delta t)$  by  $\mathbf{z}^r(\Delta t)$ . The reduced mapping obtained using the reduction–tabulation algorithm is denoted by  $\mathbf{z}_{RT}^r(\Delta t)$ .

As mentioned earlier, we consider a net reduction–tabulation error of about 2% (1% tabulation and 1% reduction) to be acceptable. In this study, we use an ISAT error tolerance of  $\epsilon_{tol} = 10^{-5}$ , which gives a tabulation error of less than 1% for both methane/air and ethylene/air premixed combustion in the PaSR. We vary the number of represented species,  $n_{rs}$ , in the RCCE method to achieve a combined reduction–tabulation error of less than 2%.

## 8. Results

In this section we present results for the partially-stirred reactor (PaSR) involving premixed combustion of (i) a methane/air mixture and (ii) an ethylene/air mixture with PaSR settings as listed in Table 1 and chemistry represented by the chemical mechanisms listed in Table 2.

We employ the previously mentioned three methods to represent chemistry – (i) ISAT with a detailed mechanism; (ii) ISAT with a skeletal or reduced mechanism; and (iii) ISAT + RCCE – and compare the reduction–tabulation errors involved in these methods.

We also compare the performance of ISAT under these various methods. To gauge the performance of ISAT under a particular method, we perform a long duration PaSR run involving over  $10^9$  queries and gather ISAT CPU time statistics. We then compute and analyze the following two quantities:

- *build time*: This is the time taken to add to and to build the table by growing EOAs. It is the total time less the time spent retrieving.
- *query time*: This is the average time taken per query after the ISAT table has been fully built with very few adds or grows being performed in the table.

Out of these two, the primary quantity of interest is the *query time*, which determines the speed of chemistry implementation i.e., the average time per reaction sub-step per particle.

### 8.1. Methane premixed combustion

In this section we present results for the methane/air premixed combustion. The PaSR computations involving premixed combustion of stoichiometric methane/air mixture are performed as described in Section 3. The chemistry is represented using the GRI-Mech 1.2 detailed and the ARM1 reduced mechanisms (details given in Table 2).

#### 8.1.1. Represented species

To select represent species for representing the chemistry with the combined ISAT–RCCE reduction–tabulation algorithm, we apply GALI on the detailed GRI-Mech 1.2 mechanism based on the reaction mapping error. The error achieved using the greedy algorithm with  $N_C = 2500$  test points and further improvement in error using the local improvement with  $N_L = 200$  test points is shown in Fig. 8. We note that for  $n_{rs} \leq 17$ , the species reconstruction error obtained by the greedy algorithm decreases exponentially with  $n_{rs}$ , and has a value of about  $10^{-3}\%$  at  $n_{rs} = 17$ . We also note that for  $n_{rs} \leq 20$ , GALI gives only marginal (less than 1%) improvement in error over the greedy algorithm at some dimensions, but at higher dimensions ( $n_{rs} > 20$ ) we see more than an order of magnitude reduction in error. At any given reduced dimension,  $n_{rs}$ , we use the species selected with GALI to perform dimension reduction with RCCE. The sets of represented species obtained using GALI for  $n_{rs} = 1–15$  are listed in Table 3.

#### 8.1.2. Reduction–tabulation error

The errors incurred for the methane/air premixed combustion with chemistry represented using the three described methods

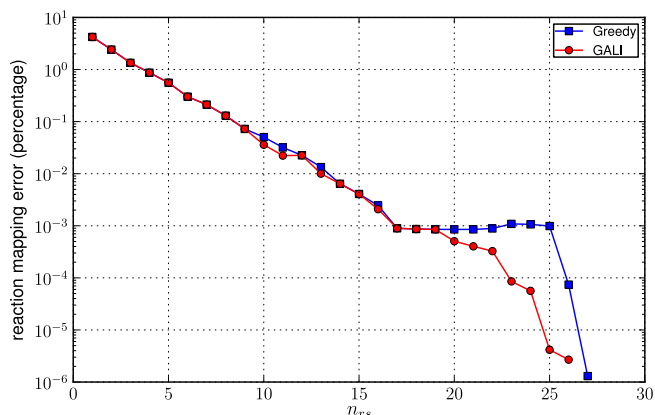


**Fig. 8.** Reaction mapping error for methane/air premixed combustion as a function of number of represented species,  $n_{rs}$ , obtained with (i) Greedy algorithm (using  $N_C = 2500$  test points) and (ii) GALI (using  $N_L = 200$  test points for local improvement). The test points are selected from a PaSR run involving methane/air premixed combustion with chemistry represented by the 31-species GRI-Mech 1.2 detailed mechanism.

**Table 3**

Sets of represented species obtained using GALI (with 31-species GRI-Mech 1.2 mechanism) for dimension reduction of methane/air premixed combustion with RCCE for  $n_{rs} = 1-15$ .

$n_{rs}$	Represented species
1	CH <sub>4</sub>
2	CH <sub>4</sub> , CO <sub>2</sub>
3	CH <sub>4</sub> , CO <sub>2</sub> , H <sub>2</sub>
4	CH <sub>4</sub> , CO <sub>2</sub> , H <sub>2</sub> , O <sub>2</sub>
5	CH <sub>4</sub> , CO <sub>2</sub> , H <sub>2</sub> , O <sub>2</sub> , H
6	CH <sub>4</sub> , CO <sub>2</sub> , H <sub>2</sub> , O <sub>2</sub> , H, OH
7	CH <sub>4</sub> , CO <sub>2</sub> , H <sub>2</sub> , O <sub>2</sub> , H, OH, O
8	CH <sub>4</sub> , CO <sub>2</sub> , H <sub>2</sub> , O <sub>2</sub> , H, OH, O, CH <sub>2</sub> O
9	CH <sub>4</sub> , CO <sub>2</sub> , H <sub>2</sub> , O <sub>2</sub> , H, OH, O, CH <sub>2</sub> O, CH <sub>3</sub>
10	CH <sub>4</sub> , CO <sub>2</sub> , H <sub>2</sub> , O <sub>2</sub> , H, OH, O, CH <sub>2</sub> O, C <sub>2</sub> H <sub>6</sub> , C <sub>2</sub> H <sub>4</sub>
11	CH <sub>4</sub> , CO <sub>2</sub> , H <sub>2</sub> , O <sub>2</sub> , H, OH, O, H <sub>2</sub> O, CH <sub>3</sub> , HO <sub>2</sub> , CO
12	CH <sub>4</sub> , CO <sub>2</sub> , H <sub>2</sub> , O <sub>2</sub> , H, OH, O, CH <sub>2</sub> O, CH <sub>3</sub> , HO <sub>2</sub> , CO, H <sub>2</sub> O
13	CH <sub>4</sub> , CO <sub>2</sub> , H <sub>2</sub> , O <sub>2</sub> , H, OH, O, CH <sub>3</sub> OH, CH <sub>3</sub> , HO <sub>2</sub> , CO, H <sub>2</sub> O, CH <sub>2</sub> CO
14	CH <sub>4</sub> , CO <sub>2</sub> , H <sub>2</sub> , O <sub>2</sub> , H, OH, O, CH <sub>2</sub> O, CH <sub>3</sub> , HO <sub>2</sub> , CO, H <sub>2</sub> O, CH <sub>2</sub> CO, C <sub>2</sub> H <sub>5</sub>
15	CH <sub>4</sub> , CO <sub>2</sub> , H <sub>2</sub> , O <sub>2</sub> , H, OH, O, CH <sub>2</sub> O, CH <sub>3</sub> , HO <sub>2</sub> , CO, H <sub>2</sub> O, CH <sub>2</sub> CO, C <sub>2</sub> H <sub>5</sub> , CH <sub>2</sub>

**Table 4**

Represented species selected using the greedy algorithm (with 111-species USC-Mech II mechanism) for dimension reduction of ethylene/air premixed combustion using RCCE for  $n_{rs} = 1-32$ .

Represented species
C <sub>2</sub> H <sub>4</sub> , O <sub>2</sub> , CO <sub>2</sub> , H <sub>2</sub> O, OH, H, CH <sub>2</sub> O, HO <sub>2</sub> , O, H <sub>2</sub> , CH <sub>4</sub> , C <sub>2</sub> H <sub>2</sub> , C <sub>2</sub> H <sub>6</sub> , H <sub>2</sub> O <sub>2</sub> , C <sub>2</sub> H <sub>3</sub> , CH <sub>2</sub> CO, C <sub>3</sub> H <sub>8</sub> , HCCO, CH <sub>2</sub> , CH <sub>3</sub> , CO, CH <sub>2</sub> CHO, C <sub>3</sub> H <sub>6</sub> , HCO, C <sub>2</sub> H <sub>5</sub> , C <sub>4</sub> H <sub>2</sub> , C <sub>4</sub> H <sub>6</sub> , CH <sub>3</sub> O, C <sub>2</sub> H, HCCOH, CH, aC <sub>3</sub> H <sub>5</sub>

are shown in Fig. 9. We see that ISAT alone with the detailed mechanism incurs about 0.1% tabulation error and ISAT with the ARM1 reduced mechanism incurs around 6% error. However, with the ISAT-RCCE methodology

- for  $n_{rs} < 10$ , the error is mainly dominated by the RCCE dimension reduction error, which decreases exponentially (similar to Fig. 8) with an increase in the number of represented species,  $n_{rs}$ , by about a factor of 10 for every 5 represented species added. (The magnitude of error in Figs. 8 and 9 are different because they are different measures of error.);
- the error is less than ISAT + REDUCED (ARM1 mechanism) with just eight or more represented species;

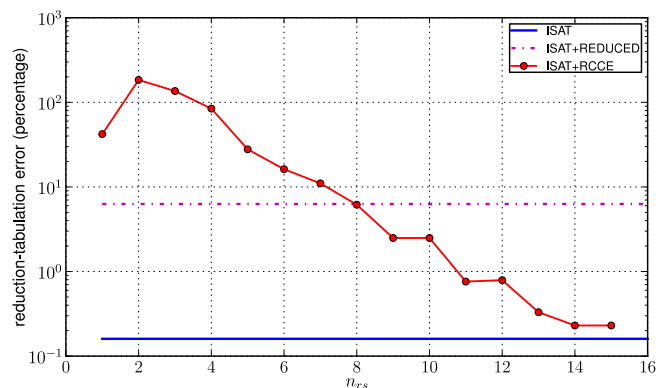


**Fig. 9.** Error incurred using (i) ISAT alone (with detailed mechanism); (ii) ISAT + REDUCED (with the ARM1 reduced mechanism); and (iii) ISAT + RCCE (using  $n_{rs}$  represented species) with chemistry represented by the detailed mechanism. The error is computed by considering  $10^5$  compositions and their reaction mappings (computed using ODE integration) obtained from a PaSR run involving methane/air premixed combustion with chemistry represented using the 31-species GRI-Mech 1.2 detailed mechanism.

- the error is less than 1% with 11 or more represented species; and
- for  $n_{rs} \geq 14$ , the error (dominantly tabulation) is comparable to ISAT alone, and hence cannot be reduced further by increasing  $n_{rs}$ .

### 8.1.3. ISAT performance

The ISAT query time for PaSR involving methane/air premixed combustion using different methods is shown in Fig. 10. The ISAT+RCCE method is used with 11 and 15 represented species (which correspond to less than 1% reduction–tabulation errors, see Fig. 9). We see that the combined reduction–tabulation algorithm provides almost twice the speedup as ISAT alone, with a query time of around 4–5  $\mu$ s, compared to 9  $\mu$ s using ISAT with the detailed mechanism. The ISAT + REDUCED query time of 5  $\mu$ s is comparable to ISAT + RCCE. The ISAT build time (estimated by the y-intercepts of dashed-lines) is about the same ( $\approx 0.6$  h) for all the methods. We also notice that ISAT+RCCE with fewer represented species yields lower query time and overall runtime because the total number of tabulated variables is reduced, and so the ISAT table size is reduced, leading to faster retrieve times.

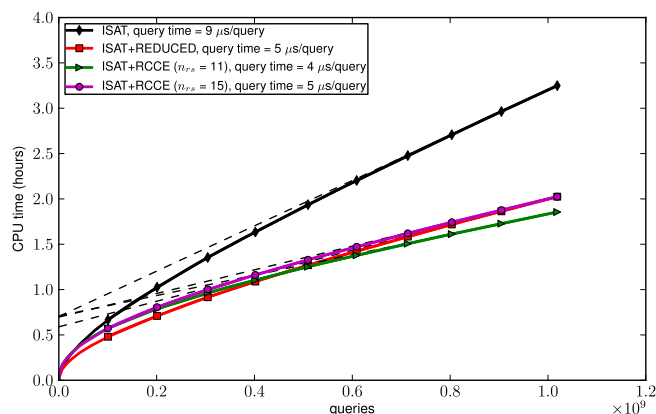


**Fig. 10.** ISAT query time for a PaSR run (with over  $10^9$  queries) involving methane/air premixed combustion using (i) ISAT (with detailed mechanism); (ii) ISAT + REDUCED (with the ARM1 reduced mechanism); and (iii) ISAT + RCCE with  $n_{rs}$  represented species and chemistry represented by the detailed mechanism. The y-intercept of linear extrapolation (dashed-line) gives an estimate of the ISAT build time for each case. The CPU time is computed by performing (serial) runs on the TACC Ranger cluster.

**Table 5**  
ISAT statistics for the methane/air premixed combustion in PaSR.

Method	$n_{rs}$	Queries ( $\times 10^9$ )	Retrieves (percentage)	Grows ( $\times 10^4$ )	Adds ( $\times 10^4$ )	Direct evals	CPU time (h)
ISAT	31	1.021	99.99	9.554	4.350	0	3.26
ISAT + REDUCED	16	1.021	99.99	10.034	4.251	0	2.03
ISAT + RCCE	11	1.021	99.99	8.265	1.892	0	1.86
ISAT + RCCE	15	1.021	99.99	8.091	1.836	0	2.03

The complete ISAT statistics for the various methods shown in Fig. 10 are listed in Table 5. We see that in all the methods 99.99% of the queries result in retrieves, which shows the efficient use of ISAT tabulation. We also note that the number of queries resulting in adds in ISAT + RCCE is less than half of that in ISAT and ISAT + REDUCED methods, which as a consequence results in relatively smaller table size and lower query time for ISAT + RCCE method.

## 8.2. Ethylene premixed combustion

In this section we present results for the ethylene/air premixed combustion. The PaSR computations involving premixed combustion of stoichiometric ethylene/air mixture are performed as described in Section 3. The chemistry is represented using USC-Mech II detailed, skeletal and reduced mechanisms (details given in Table 2).

### 8.2.1. Represented species

To select represented species for ethylene combustion, the greedy algorithm is applied on the USC-Mech II detailed mechanism. The reaction mapping error obtained using the greedy algorithm for  $n_{rs} \leq 32$  with  $N_C = 5000$  test points is shown in Fig. 11. We see that the error decreases exponentially. In the same plot, we also show the error obtained by applying the additional local improvement step using GALI over the initial few values of  $n_{rs} \leq 11$ , and we see no improvement in error except at  $n_{rs} = 3$ . Since the GALI algorithm gets expensive at higher dimensions, and we may not get significant improvement in error, so we use the species obtained using the greedy algorithm to perform dimension reduction using RCCE for ethylene combustion. The represented species obtained with the greedy algorithm for  $n_{rs} \leq 32$  are listed in Table 4.

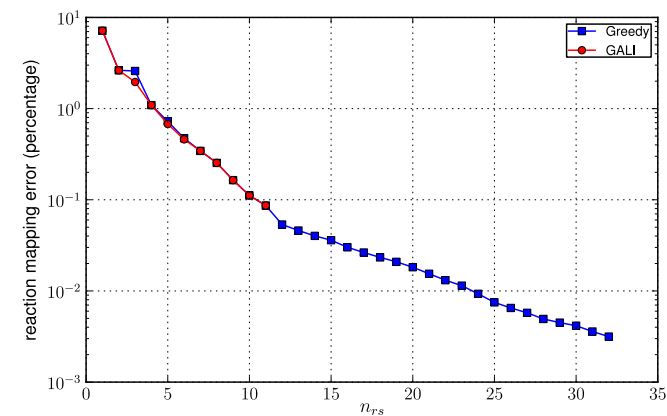


**Fig. 11.** Reaction mapping error for ethylene/air premixed combustion as a function of number of represented species,  $n_{rs}$ , obtained with (i) Greedy algorithm (using  $N_C = 5000$  test points) and (ii) GALI (at some initial values of  $n_{rs}$  using  $N_C = 500$  test points for local improvement). The test points are selected from a PaSR run involving ethylene/air premixed combustion with chemistry represented by the 111-species USC-Mech II detailed mechanism.

### 8.2.2. Reduction–tabulation error

The errors incurred for the ethylene/air premixed combustion using different methods are shown in Fig. 12. We see that ISAT alone with the detailed mechanism results in slightly less than 1% tabulation error; ISAT with the skeletal mechanism results in slightly over 3% error; and ISAT with the reduced mechanism results in slightly over 7% error. However, the combined reduction–tabulation methodology using ISAT + RCCE incurs error

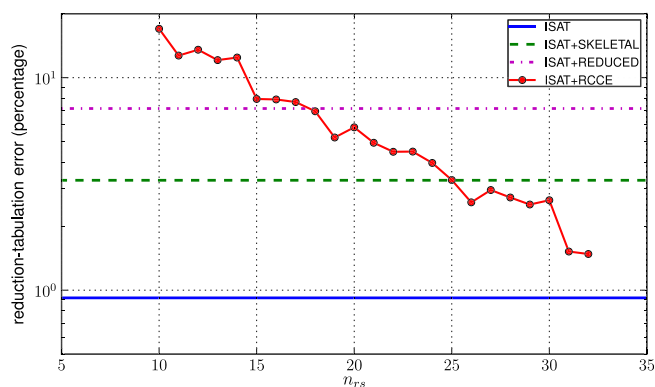


**Fig. 12.** Error incurred using (i) ISAT alone (with detailed mechanism); (ii) ISAT + SKELETAL (using ISAT with skeletal mechanism); (iii) ISAT + REDUCED (using ISAT with reduced mechanism); and (iv) ISAT + RCCE (using  $n_{rs}$  represented species) with chemistry represented by the detailed mechanism. The error is computed by considering  $10^5$  compositions and their reaction mappings (computed using ODE integration) obtained from a PaSR run involving ethylene/air premixed combustion with chemistry represented using the 111-species USC-Mech II detailed mechanism.

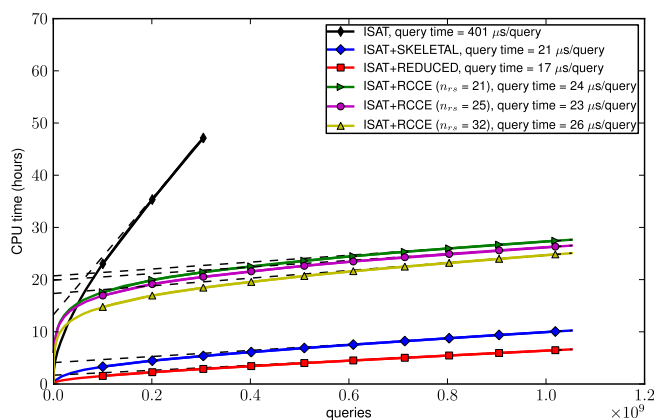


**Fig. 13.** ISAT query time for a PaSR run (of maximum 48 h with over  $10^9$  queries) involving ethylene/air premixed combustion using (i) ISAT (with detailed mechanism); (ii) ISAT + SKELETAL (using ISAT with skeletal mechanism); (iii) ISAT + REDUCED (using ISAT with reduced mechanism); and (iv) ISAT + RCCE with  $n_{rs}$  represented species and chemistry represented by the detailed mechanism. The y-intercept of linear extrapolation (dashed-line) gives an estimate of the ISAT build time for each case. The CPU time is computed by performing (serial) runs on the TACC Ranger cluster.

**Table 6**

ISAT statistics for the ethylene/air premixed combustion in PaSR.

Method	$n_{rs}$	Queries ( $\times 10^9$ )	Retrieves (percentage)	Grows ( $\times 10^5$ )	Adds ( $\times 10^4$ )	Direct evals ( $\times 10^6$ )	CPU time (h)
ISAT	111	0.304	99.49	1.447	0.498	1.392	47.12
ISAT + SKELETAL	38	1.052	99.94	5.070	3.692	0.125	10.25
ISAT + REDUCED	24	1.052	99.95	4.565	7.658	0	6.64
ISAT + RCCE	21	1.052	99.97	2.927	3.010	0	27.65
ISAT + RCCE	25	1.052	99.97	3.005	2.806	0	26.53
ISAT + RCCE	32	1.052	99.97	2.675	2.559	0	25.07

- less than ISAT + REDUCED with just 18 or more represented species; and
- less than ISAT + SKELETAL with just 25 or more represented species; and
- less than 2% error with 31 or more represented species,

which shows that the combined reduction–tabulation approach shows good error control even with relatively large mechanisms involving more than 100 species.

### 8.2.3. ISAT performance

The query time computed for PaSR involving ethylene/air premixed combustion is shown in Fig. 13. Here the ISAT + RCCE is tested with 21, 25 and 32 represented species (which correspond to about 5%, 3% and 1% reduction–tabulation errors respectively, see Fig. 12). We see that ISAT–RCCE provides more than 15-fold speedup, with a query time of around 24  $\mu$ s compared to 400  $\mu$ s using ISAT alone with the detailed mechanism. The query times for ISAT + RCCE are comparable to ISAT + SKELETAL/REDUCED query times. In this case, the build times for ISAT + RCCE (around 20 h) are significantly higher than for ISAT + SKELETAL/REDUCED (about 3 h), owing to the expensive adds performed in ISAT + RCCE in the initial stages which involve species reconstruction and evaluation of reaction mapping based on the detailed mechanism (as described in Section 5.1). However, when applied to LES/PDF computations which require  $\mathcal{O}(10^5)$  CPU hours, the build time for ISAT + RCCE is still insignificant; and typically for such large runs, the ISAT table can be built once, saved and reused for later computations.

In this case with ISAT–RCCE (unlike for the methane/air premixed combustion in Fig. 10) we notice that:

1. the query time does not consistently decrease as the number of represented species is reduced; and
2. the overall runtime increases as the number of represented species is reduced.

This is presumably because the ISAT tables in the ISAT–RCCE cases have not have been fully built yet due to the large build time of around 20 h. The estimates for the query time for such a short run may not be very accurate. As the number of represented species is reduced, we should expect to see a reduction in the query time (and thus the overall runtime) for longer runs involving  $10^{11}$ – $10^{12}$  queries.

The full ISAT statistics for the various runs shown in Fig. 13 are listed in Table 6. We again see that in all the methods more than 99.4% of the queries result in retrieves showing the high efficiency of ISAT tabulation. In this case, owing to the large number of species present in the detailed (111-species) and skeletal (38-species) mechanisms, the ISAT table size (1 GB) gets filled up quickly in the ISAT and ISAT + SKELETAL methods, resulting in direct evaluation (DE) of the unresolved queries using the expensive ODE integration. For ISAT alone and ISAT + SKELETAL methods, more than 1.4 and 0.1 million queries result in DEs, respectively. Here again, we note that ISAT + RCCE results in relatively fewer adds compared

to the combined adds + DEs in ISAT alone and ISAT + SKELETAL/REDUCED methods.

## 9. Conclusions

Based on the results presented here, we can draw the following conclusions:

- The reduction–tabulation error results show that the combined ISAT–RCCE–GALI algorithm can achieve errors comparable to ISAT alone (in this case for  $\epsilon_{tol} = 10^{-5}$ ) using a relatively small number of represented species: 14 out of 31 species for the methane/air premixed case (see Fig. 9) and 32 out of 111 species for the ethylene/air premixed combustion (see Fig. 12).
- The ISAT–RCCE–GALI algorithm is also seen to achieve reduction–tabulation errors lower than ISAT with skeletal or reduced mechanisms with relatively fewer number of represented species. In methane/air premixed combustion, ISAT + REDUCED (16-species ARM1) error is achieved with ISAT–RCCE with just 8 or more represented species (see Fig. 9); and in ethylene/air premixed combustion, ISAT–REDUCED (24-species) and ISAT–SKELETAL (38-species) errors are achieved with ISAT–RCCE with just 18 and 25 represented species, respectively (see Fig. 12).
- The ISAT–RCCE–GALI algorithm is also computationally efficient resulting in a query time of around 4  $\mu$ s (twofold speedup) for the methane/air premixed combustion using 11–15 represented species compared to 9  $\mu$ s using ISAT with 31-species detailed mechanism (see Fig. 10); and a query time of around 24  $\mu$ s (15-fold speedup) for ethylene/air premixed combustion using 21–32 represented species compared to 400  $\mu$ s using ISAT with 111-species detailed mechanism (see Fig. 13).
- The combined approach shows both good error control and performance. With fewer species to track in the CFD code, this combined ISAT–RCCE–GALI approach provides a computationally accurate and efficient way of representing combustion chemistry.

Here, we would also like to mention that the combined reduction–tabulation procedure described in this work can also be used with the ICE–PIC dimension reduction method [13,23]. The GALI algorithm can be used to select represented species for ICE–PIC and the combined ISAT–ICE–PIC–GALI approach can be applied for representing combustion chemistry.

## Acknowledgments

This work is supported in part by Department of Energy under Grant DE-FG02-90ER and by Grant Number FA9550-09-1-0611 funded by AFOSR and NASA ARMD, technical monitors Julian Tishkoff (AFOSR) and Aaron Auslender and Rick Gaffney (NASA). We are grateful to Jon Kleinberg for discussions on local improvement algorithm for GALI. SBP has a financial interest in Ithaca Combustion Enterprise, LLC., which has licensed the software ISAT–CK and CEQ used in this work.

## Appendix A. Approximation of temperature and density

In this section we describe how the temperature and density are approximated using the reduced representation in the reduction-tabulation algorithm.

### A.1. Approximation of temperature

In the full composition space, given the composition  $\mathbf{z} = \{\mathbf{z}^r, \mathbf{z}^u\}$  and temperature  $T$ , the enthalpy  $h$  is given as

$$h(\mathbf{z}, T) = \mathbf{h}^T(T)\mathbf{z} = \mathbf{h}^{rT}(T)\mathbf{z}^r + \mathbf{h}^{uT}(T)\mathbf{z}^u = h^r + h^u, \quad (17)$$

where  $\mathbf{h}$  denotes molar enthalpies of species, and the superscripts  $r$  and  $u$  denote the represented and unrepresented components.

Given the full composition  $\mathbf{z}$  and the total enthalpy  $h$ , the temperature  $T$  is computed using Newton's method which satisfies the following equation:

$$h = h(\mathbf{z}, T). \quad (18)$$

However, with dimension reduction, only the composition of represented species are stored in the reduced representation,  $\mathbf{r} = \{\mathbf{z}^r, \mathbf{z}^{u,e}\}$ . So, given the reduced representation  $\mathbf{r}$  and temperature  $T$ , the represented part of enthalpy,  $h^r$ , can be computed exactly, but  $h^u$  needs to be approximated. Let the approximated total enthalpy,  $h^a$ , be given as

$$h^a(\mathbf{r}, T) = \mathbf{h}^{rT}(T)\mathbf{z}^r + (\mathbf{h}^{uT}(T)\mathbf{P})(\mathbf{E}^{uT}\mathbf{z}^u) = h^r + \mathbf{h}^{uT}(T)\mathbf{P}\mathbf{z}^{u,e}, \quad (19)$$

where  $\mathbf{E}^u$  is the constant  $n_{us} \times n_e$  element matrix for unrepresented species such that  $\mathbf{z}^{u,e} = \mathbf{E}^{uT}\mathbf{z}^u$ , and  $\mathbf{P}$  is a specified constant  $n_{us} \times n_e$  matrix. The question now to be addressed is: how best to specify  $\mathbf{P}$ ? In the above approximation for enthalpy, we are implicitly approximating  $\mathbf{z}^u$  and  $h^u$  as

$$\mathbf{z}^{u,a} \equiv \mathbf{P}\mathbf{z}^{u,e}, \quad (20)$$

$$h^{u,a} \equiv \mathbf{h}^{uT}(T)\mathbf{z}^{u,a}, \quad (21)$$

which gives

$$h^a = h^r + h^{u,a}. \quad (22)$$

In the above approximation, it is important to note that

- $\mathbf{z}^{u,a}$  may not be realizable.
- $\mathbf{z}^{u,a}$  is used only to estimate  $h$ ,  $\rho$  and  $T$ , and not to approximate  $\mathbf{z}^u$  directly.

Note that one possible way of computing  $\mathbf{z}^{u,a}$  is by performing a constrained-equilibrium calculation, but this is relatively expensive and takes  $\mathcal{O}(10^3)$   $\mu\text{s}$  compared to a typical query time of  $\mathcal{O}(10)$   $\mu\text{s}$ , and hence is avoided.

We define the approximation error in  $\mathbf{z}^{u,a}$  as

$$\delta\mathbf{z}^{u,a} = \mathbf{z}^{u,a} - \mathbf{z}^u, \quad (23)$$

and the approximation error in enthalpy as

$$\delta h = h^a - h = h^{u,a} - h^u = \mathbf{h}^{uT}(T)(\mathbf{P}\mathbf{E}^{uT} - \mathbf{I})\mathbf{z}^u. \quad (24)$$

For a given reduced representation,  $\mathbf{r} = \{\mathbf{z}^r, \mathbf{z}^{u,e}\}$ , and enthalpy,  $h$ , the approximate temperature,  $T^a$  is defined as

$$h = h^a(\mathbf{r}, T^a), \quad (25)$$

which is computed using Newton's method.

In the next two subsections we describe two different methods for computing the matrix  $\mathbf{P}$  for approximating the enthalpy,  $h^a$  using Eq. (19).

### A.1.1. Method 1

If  $\mathbf{z}^u$  is not known, then the best approximation for  $\mathbf{P}$  that minimizes the error (Eq. (24)) in the approximated enthalpy,  $h^a$ , is obtained by setting  $\mathbf{P}$  equal to the pseudo-inverse of  $\mathbf{E}^{uT}$ . Let  $\mathbf{P} = \mathbf{P}_1 = \text{pseudo-inverse}(\mathbf{E}^{uT})$ , computed using the SVD of  $\mathbf{E}^{uT}$ .

### A.1.2. Method 2

Assuming  $\mathbf{z}^u$  is known at  $N$  test points, an improved approximation for enthalpy can be computed using this known information. Let the values of  $\mathbf{z}^u$  computed at these  $N$  test points be stored in an  $n_{us} \times N$  matrix,  $\mathbf{Z}^u$ . The error in the approximated enthalpy,  $h^a$  computed at the  $i^{\text{th}}$  test point is given (in an obvious notation) as

$$\delta h_i = \mathbf{h}_i^{uT}(T)(\mathbf{P}\mathbf{E}^{uT} - \mathbf{I})\mathbf{z}_i^u. \quad (26)$$

The vector  $\mathbf{h}_i^{uT}(T)$  is different for each test point and depends on the temperature at that point. Minimizing the overall error in the approximated enthalpy at all the test points using the above equation is not easy, and so we instead minimize the error in approximating  $\mathbf{z}^u$  given as

$$\delta\mathbf{z}_i^{u,a} = \mathbf{z}_i^{u,a} - \mathbf{z}_i^u = (\mathbf{P}\mathbf{E}^{uT} - \mathbf{I})\mathbf{z}_i^u. \quad (27)$$

Based on this error, the error in the approximated  $\mathbf{z}^u$  at all the  $N$  test points is denoted by the  $n_{us} \times N$  matrix  $\delta\mathbf{Z}^{u,a}$  and is given as

$$\delta\mathbf{Z}^{u,a} = \mathbf{P}\mathbf{E}^{uT}\mathbf{Z}^u - \mathbf{Z}^u. \quad (28)$$

We compute  $\mathbf{P}$  which minimizes the error,  $\|\delta\mathbf{Z}^{u,a}\|_2$  as follows. Let the SVD of  $\mathbf{Z}^u$  be given as

$$\mathbf{Z}^u = \mathbf{U}\mathbf{\Sigma}\mathbf{V}^T, \quad (29)$$

and let the first  $n_e$  vectors of  $\mathbf{U}$  be denoted by the  $n_{us} \times n_e$  matrix  $\mathbf{X}$ . Then the matrix  $\mathbf{P} \equiv \mathbf{P}_2$ , which minimizes the error  $\|\delta\mathbf{Z}^{u,a}\|_2$  (Eq. (28)) is given as

$$\mathbf{P}_2 = \mathbf{X}(\mathbf{E}^{uT}\mathbf{X})^{-1}. \quad (30)$$

So, we have two methods for computing the matrix  $\mathbf{P}$  to approximate the enthalpy and thus temperature:

1.  $\mathbf{P} = \mathbf{P}_1$  – easily computable, but not very accurate
2.  $\mathbf{P} = \mathbf{P}_2$  – accurate but requires some stored values of  $\mathbf{z}^u$

In our current implementation, we start the computations by setting  $\mathbf{P} = \mathbf{P}_1$  and start storing  $\mathbf{z}^u$  values as they are computed. After a certain number of  $\mathbf{z}^u$  values have been stored, based on some error criterion, the matrix  $\mathbf{P}$  is reset to  $\mathbf{P}_2$ .

### A.2. Approximation of density

Given the full composition  $\mathbf{z} = \{\mathbf{z}^r, \mathbf{z}^u\}$ , the density,  $\rho$ , is computed using the ideal gas law as follows:

$$\rho = \frac{p}{R_u T \sum_{i=1}^{n_s} Z_i}, \quad (31)$$

where  $p$  is the pressure.

However, with dimension reduction, given only the reduced representation,  $\mathbf{r}$ , the sum  $\sum_{i=1}^{n_s} Z_i$  is approximated as

$$\sum_{i=1}^{n_s} Z_i^a \equiv \sum_{i=1}^{n_{rs}} Z_i^r + \sum_{i=1}^{n_{us}} Z_i^{u,a}, \quad (32)$$

and the approximated density,  $\rho^a$  is given as

$$\rho^a = \frac{p}{R_u T^a \sum_{i=1}^{n_s} Z_i^a}. \quad (33)$$

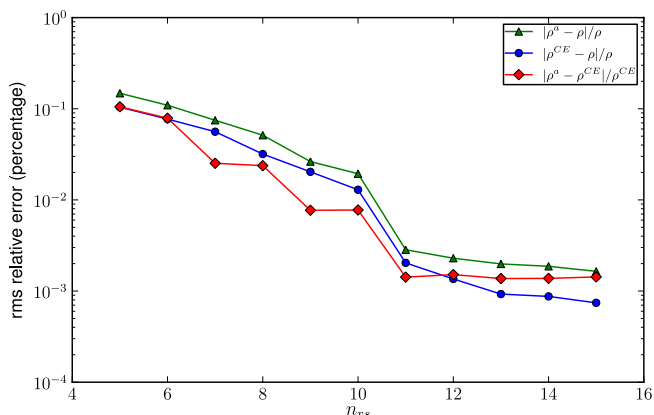


**Fig. 14.** The root-mean-square relative error in the approximated density,  $\rho^a$ , (computed using the RCCE reduced representation for methane/air premixed combustion at various values of  $n_{rs}$ ) relative to the exact density,  $\rho$ , and the density computed using a (relatively expensive) constrained-equilibrium reconstruction,  $\rho^{CE}$ . The errors are computed by considering  $10^5$  test compositions in the full composition space from a methane/air premixed combustion in PaSR.

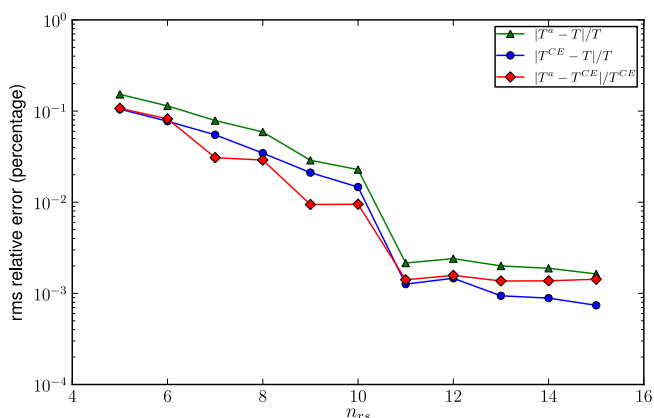


**Fig. 15.** The root-mean-square relative error in the approximated temperature,  $T^a$ , (computed using the RCCE reduced representation for methane/air premixed combustion at various values of  $n_{rs}$ ) relative to the exact temperature,  $T$ , and the temperature computed using a (relatively expensive) constrained-equilibrium reconstruction,  $T^{CE}$ . The errors are computed by considering  $10^5$  test compositions in the full composition space from a methane/air premixed combustion in PaSR.

### A.3. Approximation errors

The approximation errors in temperature and density are computed by considering  $10^5$  test compositions from a methane/air premixed combustion in the PaSR. The results are shown in Figs. 14 and 15. We see that less than 1% root-mean-square relative error is measured in the approximated density and temperature relative to the exact values and those computed using the constrained-equilibrium reconstruction, which is more than two orders of

magnitude more expensive than a typical ISAT query time and hence is avoided. The time spent in approximating the temperature and density using the aforementioned method is negligible compared to the ISAT query time. We also note that in general the approximation error reduces as the number of represented species,  $n_{rs}$ , is increased.

### References

- [1] W.J. Pitz, N.P. Cernansky, F.L. Dryer, F.N. Egolfopoulos, J.T. Farrell, D.G. Friend, H. Pitsch, Society of Automotive Engineers SAE-2007-01-0175 (2007).
- [2] C.K. Westbrook, W.J. Pitz, O. Herbinet, H.J. Curran, E.J. Silke, Combust. Flame 156 (2009) 181–199.
- [3] T. Lu, C.K. Law, Proc. Combust. Inst. 30 (2005) 1333–1341.
- [4] P. Pepiot-Desjardins, H. Pitsch, Combust. Flame 154 (2008) 67–81.
- [5] T. Nagy, T. Turanyi, Combust. Flame 156 (2009) 417–428.
- [6] M. Bodenstein, S.C. Lind, Z. Phys. Chem. 57 (1906) 168.
- [7] M.D. Smooke, Reduced Kinetic Mechanisms and Asymptotic Approximations for Methane–Air Flames, Springer-Verlag, Berlin, 1991.
- [8] J.C. Keck, D. Gillespie, Combust. Flame 17 (1971) 237–241.
- [9] J.C. Keck, Prog. Energy Combust. Sci. 16 (1990) 125–154.
- [10] S.H. Lam, D.A. Goussis, Int. J. Chem. Kinet. 26 (1994) 461–486.
- [11] U. Maas, S.B. Pope, Combust. Flame 88 (1992) 239–264.
- [12] S.B. Pope, U. Mass, Mechanical and Aerospace Engineering Report FDA 93-11, Cornell University, Ithaca, 1993.
- [13] Z. Ren, S.B. Pope, A. Vladimirov, J.M. Guckenheimer, J. Chem. Phys. 124 (2006) (Art. No. 114111).
- [14] A.N. Al-Khateeb, J.M. Powers, S. Paolucci, A.J. Sommes, J.A. Diller, J.D. Hauenstein, J.D. Mengers, J. Chem. Phys. 131 (2009) 024118 (1–19).
- [15] J.-Y. Chen, W. Kollmann, R.W. Dibble, Combust. Sci. Technol. 64 (1989) 315–346.
- [16] T. Turanyi, Comput. Chem. 18 (1994) 45–54.
- [17] F.C. Christo, A.R. Masri, E.M. Nebot, S.B. Pope, Proc. Combust. Inst. 26 (1996) 43–48.
- [18] S.B. Pope, Combust. Theory Modell. 1 (1997) 41–63.
- [19] L. Lu, S.B. Pope, J. Comput. Phys. 228 (2) (2009) 361–386.
- [20] S.R. Tonse, N.W. Moriarthy, N.J. Brown, M. Frenklach, Isr. J. Chem. 39 (1999) 97–106.
- [21] Q. Tang, J. Xu, S.B. Pope, Proc. Combust. Inst. 28 (2000) 133–139.
- [22] Q. Tang, S.B. Pope, Proc. Combust. Inst. 29 (2002) 1411–1417.
- [23] Z. Ren, V. Hiremath, S.B. Pope, 6th US National Combustion Meeting, May 17–20, 2009, Ann Arbor, Michigan, 2009.
- [24] S.B. Pope, Prog. Energy Combust. Sci. 11 (1985) 119–192.
- [25] Z. Ren, V. Hiremath, S.B. Pope (2009). <<http://eccentric.mae.cornell.edu/~tcg/ice-pic>>.
- [26] V. Hiremath, Z. Ren, S.B. Pope, Combust. Theory Modell. 14 (5) (2010) 619–652.
- [27] M. Caracotsios, W.E. Stewart, Comput. Chem. Eng. 9 (1985) 359–365.
- [28] M. Sandip, J. Heat Transfer 129 (2007) 526–535.
- [29] J.D. Hedengren, T.F. Edgar, Comput. Chem. Eng. 32 (2008) 706–714.
- [30] M. Janbozorgi, H. Metghalchi, Int. J. Thermodyn. 12 (2009) 44–50.
- [31] M. Janbozorgi, S. Ugarte, H. Metghalchi, J.C. Keck, Combust. Flame 156 (2009) 1871–1885.
- [32] S.B. Pope, Combust. Flame 139 (2004) 222–226.
- [33] D. Hamiroune, P. Bishnu, M. Metghalchi, J.C. Keck, Combust. Theory Modell. 2 (1998) 81–94.
- [34] T.H. Cormen, C.E. Leiserson, R.L. Rivest, C. Stein, Introduction to Algorithms, MIT Press, and McGraw-Hill, 2001.
- [35] M. Frenklach, H. Wang, C.-L. Yu, M. Goldenberg, C. Bowman, R. Hanson, D. Davidson, E. Chang, G. Smith, D. Golden, W. Gardiner, V. Lissianski (1995). <[http://www.me.berkeley.edu/gri\\_mech/](http://www.me.berkeley.edu/gri_mech/)>.
- [36] C.J. Sung, C.K. Law, J.-Y. Chen, Symp. (Int.) Combust. 27 (1998) 295–304. <<http://www.princeton.edu/~cklaw/kinetics/12-step/index.html>>.
- [37] H. Wang, X. You, A.V. Joshi, S.G. Davis, A. Laskin, F. Egolfopoulos, C.K. Law (May 2007). <[http://ignis.usc.edu/USC\\_Mech\\_IL.htm](http://ignis.usc.edu/USC_Mech_IL.htm)>.
- [38] D.A. Sheen, X. You, H. Wang, T. Lovas, Proc. Combust. Inst. 32 (2009) 535–542.
- [39] G.E. Esposito, H.K. Chelliah, Combust. Flame 158 (3) (2011) 477–489.
- [40] A.C. Zambon, H.K. Chelliah, Combust. Flame 150 (2007) 71–91.